

# Magnetohydrodynamics natural convection of nanofluid flow over a vertical circular cone embedded in a porous medium and subjected to thermal radiation

## Abstract

In this paper, magnetohydrodynamics natural convection of nanofluid flow over a vertical circular cone immersed in a porous medium under the influence of thermal radiation is investigated using multi-step differential transformation method. The accuracies of the analytical solutions are established through the verifications of the results of the present study with the results of the numerical solutions and the past studies. The approximate analytical solutions are used to examine the impacts of cone angle, flow medium porosity, magnetic field, nanoparticles volume-fraction and shape on the flow and heat transfer behaviours of the Copper (II) Oxide-water nanofluid. It is hoped that this study will enhance better understanding of flow process for the design of flow and heat transfer equipment.

**Keywords:** free convection, cone angle, porous medium, nanoparticle, magnetic field, multi-step differential transformation method

Volume 5 Issue 1 - 2020

**MG Sobamowo, AA Yinusa, ST Aladenusi, MO Salami**

Department of Mechanical Engineering, University of Lagos, Nigeria

**Correspondence:** MG Sobamowo, Department of Mechanical Engineering, University of Lagos, Akoka, Lagos, Nigeria, Email [mikegeminiyi@gmail.com](mailto:mikegeminiyi@gmail.com)

**Received:** January 01, 2020 | **Published:** July 14, 2020

**Nomenclature:**  $c_p$ , specific heat capacity;  $k$ , thermal conductivity;  $m$ , shape factor;  $Pr$ , Prandtl number;  $u$ , velocity component in x-direction;  $v$ , velocity component in z-direction;  $y$ , axis perpendicular to plates;  $x$ , axis along the horizontal direction;  $y$ , axis along the vertical direction

**Symbols:**  $\beta$ , volumetric extension coefficients;  $\rho$ , density of the fluid;  $\mu$ , dynamic viscosity;  $\eta$ , similarity variable;  $\lambda$ , sphericity;  $\phi$ , volume fraction or concentration of the nanofluid;  $\theta$ , dimensionless temperature

**Subscript:** f, fluid; s, solid; nf, nanofluid

## Introduction

There are various applications of free convection flow and heat transfer in aeronautics, reactor fluidization, glass-fiber production processes, aerodynamic, cooling of gas turbine rotor blades, drawing of a polymer sheet, food stuff processing, melt spinning, mechanical forming processes, cooling of metallic plates, wire and fiber coating, extrusion of plastic sheets, continuous casting, rolling, annealing, and tinning of copper wires. Since the quality of products in the processes depends considerably on the flow and heat transfer characteristics in the various applications, the analysis of fluid flow and heat transfer is very essential. Earlier studies on free convections flow established its importance in science and engineering applications.<sup>1-11</sup> However, the analyses of these studies are based on the approximations. Therefore, in some recent studies, improved approximated analyses of the flow and heat transfer models have been presented. Na & Habib<sup>12</sup> adopted parameter differentiation method while Merkin<sup>13</sup> presented the similarity solutions for free convection on a vertical plate. Merkin & Pop<sup>14</sup> and Ali et al.,<sup>15</sup> applied numerical methods for the flow process. In a very recent paper, Motsa et al.,<sup>16,17</sup> utilized homotopy analysis method and spectral local linearization approach to analyze the free

convection boundary layer flow with heat and mass transfer. Also, Ghotbi et al.,<sup>18</sup> presented the analytical solutions to the free convection flow using the homotopy analysis method.

The simple procedures in the theory and applications of differential transformation method (DTM) have shown the effectiveness of the method in solving both linear and nonlinear equations. The method was introduced by Zhou.<sup>19</sup> In the free flow analysis, over a vertical surface, Yu & Chen<sup>20</sup> and Kuo<sup>21,22</sup> applied the method. However, it should be noted that the DTM solutions diverge for some differential equations that extremely have nonlinear behaviors or have boundary-conditions at infinity. This is because the series solution method is limited to small domain. Therefore, Rashidi et al.,<sup>23</sup> applied DTM coupled with Padé-approximant technique to the flow problem. However, the Padé-approximant technique comes with large volume of calculations and computations. Therefore, another technique for an improved rate of convergence and the radius of convergence of power series solution is required. Among the newly developed techniques, is the multi-step differential transform method (MDTM). The method can be applied directly to nonlinear differential equations of infinite boundary conditions without the use of after-treatment techniques and domain transformation techniques.<sup>24-44</sup>

The previous studies on the problem under investigation are based on the flow of viscous fluid over a vertical surface without considering the effects of magnetic field and porosity of the flow medium. To the best of the author's knowledge, a study on free convection flow of nanofluid over a vertical circular cone using multi-step differential transform method. Therefore, in this work, magnetohydrodynamics natural convection of nanofluid flow over a vertical circular cone immersed in a porous medium under the influence of thermal radiation is investigated using multi-step differential transformation method. The approximate analytical solutions are used to examine the impacts of cone angle, flow medium porosity, magnetic field, nanoparticles volume-fraction, shape and type on the flow and heat

transfer behaviours of various nanofluids. Also, the accuracies of the analytical solutions are established through the verifications of the results with the results of the numerical solutions and the results in the past studies.

### Problem formulation and mathematical analysis

Consider a free-convection flow of an incompressible electrically conducting nanofluid past a cone embedded in a porous medium which is inclined from the vertical with an acute angle  $\gamma$  measured in the clockwise direction and situated in an otherwise quiescent ambient fluid at temperature  $T_w$  as shown in Figure 1. A transverse magnetic field of strength  $B_0$  is applied normal to the inclined plate. The plate coincides with the plane  $y=0$  and the flow being confined to  $y>0$ . Assuming that the flow in the laminar boundary layer is two-dimensional and steady, the equations for continuity and motion are given as

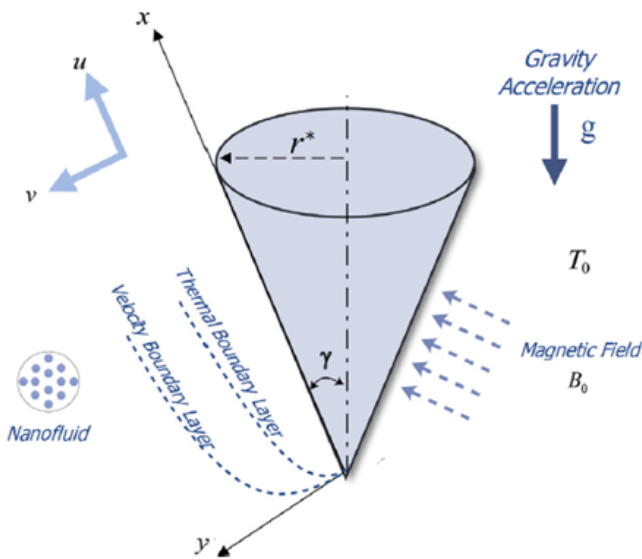


**Figure 1** The geometry of the of the free convection flow over the cone.

$$\frac{\partial(ru)}{\partial x} + \frac{\partial(rv)}{\partial y} = 0 \quad (1)$$

$$\rho_{nf} \left( u \frac{\partial u}{\partial x} + v \frac{\partial u}{\partial y} \right) = \mu_{nf} \frac{\partial^2 u}{\partial y^2} + g(\rho\beta)_{nf} (T - T_\infty) \cos \gamma - \sigma B_0^2 u - \frac{\mu u}{K} \quad (2)$$

$$(\rho c_p)_{nf} \left( u \frac{\partial T}{\partial x} + v \frac{\partial T}{\partial y} \right) = k_{nf} \frac{\partial^2 T}{\partial y^2} - \frac{\partial q_r}{\partial y} \quad (3)$$

Assuming no slip conditions, the appropriate boundary conditions are given as

$$u = 0, \quad v = 0, \quad T = T_s \quad \text{at} \quad y = 0 \quad (4a)$$

$$u = 0, \quad T = T_w, \quad \text{at} \quad y \rightarrow \infty \quad (4b)$$

where the various physical and thermal properties in the Eq. (1-3) are given as

$$\rho_{nf} = \rho_f (1 - \phi) + \rho_s \phi \quad (5a)$$

$$(\rho c_p)_{nf} = (\rho c_p)_f (1 - \phi) + (\rho c_p)_s \phi \quad (5b)$$

$$(\rho\beta)_{nf} = (\rho\beta)_f (1 - \phi) + (\rho\beta)_s \phi \quad (5c)$$

$$\mu_{nf} = \frac{\mu_f}{(1 - \phi)^{2.5}} \quad (5d)$$

$$k_{nf} = k_f \left[ \frac{k_s + (m - 1)k_f - (m - 1)\phi(k_f - k_s)}{k_s + (m - 1)k_f + \phi(k_f - k_s)} \right] \quad (6)$$

$$\sigma_{nf} = \sigma_f \left[ 1 + \frac{3 \left\{ \frac{\sigma_s}{\sigma_f} - 1 \right\} \phi}{\left\{ \frac{\sigma_s}{\sigma_f} + 2 \right\} \phi - \left\{ \frac{\sigma_s}{\sigma_f} - 1 \right\} \phi} \right] \quad (7)$$

The above model in Eq. (6) is Hamilton Crosser's model. The "m" in the model represents the shape factor which its numerical values for different shapes are given in Table 1. It should be noted that the shape factor,  $m = \frac{3}{\lambda}$ , where  $\lambda$  is the sphericity (the ratio of the surface area of the sphere and the surface area of the real particles with equal volumes). For sphericity of sphere, platelet, cylinder, laminar and brick are 1.000, 0.526, 0.625, 0.185 and 0.811, respectively. It should be noted that the Hamilton Crosser's model becomes a Maxwell-Garnett's model, when the shape factor of the nanoparticle,  $m=3$ . Tables 2&3 present the physical and thermal properties of the base fluid and the nanoparticles, respectively. SWCNTs mean single-walled carbon nanotubes.

However, the present study focusses on Copper (II) Oxide-water nanofluid.

$$r = x \sin \lambda, \quad (8)$$

Moreover  $\gamma$  is the half angle of the frustum cone. Because the boundary layer-thickness is small, the local radius to a point in the boundary layer  $r$  can be represented by the local radius of the cone.

Going back to Eq. (1), (2) and (3) and if one introduces a stream function,  $\psi(x, y)$  such that





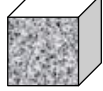
$$ru = \frac{\partial \psi}{\partial y}, \quad rv = -\frac{\partial \psi}{\partial x}, \quad (9)$$

and use the following similarity and dimensionless variables

$$\eta = \left[ \frac{\rho_f^2 (g \beta_f (T_w - T_\infty))}{4 \mu_f^2 x} \right]^{1/4} y, \quad \psi = \frac{4 \mu_f}{\rho_f} \left[ \frac{\rho_f^2 (g \beta_f (T_w - T_\infty)) x^3}{4 \mu_f^2} \right]^{1/4} f(\eta), \quad \theta = \frac{T - T_\infty}{T_w - T_\infty}, \quad Pr = \frac{\mu_f c_p}{k_f}, \quad (10)$$

one arrives at fully coupled third and second orders ordinary differential equations

**Table 1** The values of different shapes of nanoparticles<sup>37,38</sup>

S/N	Name	Shape	Shape factor (m)	Sphericity( $\psi$ )
1	Sphere		3.0	1.000
2	Platelet		5.7	0.526
3	Cylinder		4.8	0.625
4	Lamina		16.2	0.185
5	Brick		3.7	0.811

**Table 2** Physical and thermal properties of the base fluid<sup>37-44</sup>

Base fluid	$\rho$ (kg/m <sup>3</sup> )	$c_p$ (J/kgK)	k (W/mK)
Pure water	997.1	4179	0.613
Ethylene Glycol	1115	2430	0.253
Engine oil	884	1910	0.144
Kerosene	783	2010	0.145

**Table 3** Physical and thermal properties of nanoparticles<sup>37-44</sup>

Nanoparticles	$\rho$ (kg/m <sup>3</sup> )	$c_p$ (J/kgK)	k (W/mK)
Copper (Cu)	8933	385	401
Aluminum oxide (Al <sub>2</sub> O <sub>3</sub> )	3970	765	40
SWCNTs	2600	42.5	6600
Silver (Ag)	10500	235	429
Titanium dioxide (TiO <sub>2</sub> )	4250	686.2	8.9538
Copper (II) Oxide (CuO)	783	540	18

$$f'''(\eta) + (1-\phi)^{2.5} \left\{ \left[ (1-\phi) + \phi \left( \frac{\rho_s}{\rho_f} \right) \right] \left( 3f(\eta)f''(\eta) - 2(f'(\eta))^2 \right) \right. \\ \left. + \left[ (1-\phi) + \phi \left[ (\rho\beta)_s / (\rho\beta)_f \right] \right] \theta(\eta) \cos \gamma \right\} - \left( M^2 + \frac{1}{Da} \right) f(\eta) = 0$$

$$\left( 1 + \frac{4}{3}R \right) \theta'' + 3 \left[ \frac{1}{(1-\phi) + \phi \left[ (\rho C_p)_s / (\rho C_p)_f \right]} \left[ \frac{k_s + (m-1)k_f - (m-1)\phi(k_f - k_s)}{(12)} + (m-1)k_f + \phi(k_f - k_s) \right] \right] Prf \theta' = 0$$

and the boundary conditions as

$$f = 0, \quad f' = 0, \quad \theta = 1, \quad \text{when } \eta = 0 \quad (13)$$

$$f' = 0, \quad \theta = 0, \quad \text{when } \eta = \infty \quad (14)$$

### Basic concepts of differential transform method

The relatively new semi-analytical method, differential transformation method introduced by Zhou<sup>19</sup> has proven proved very effective in providing highly accurate solutions to differential

equations, difference equation, differential-difference equations, fractional differential equation, pantograph equation and integro-differential equation. Therefore, this method is applied to the present study. The basic definitions and the operational properties of the method are as follows

If  $u(t)$  is analytic in the domain  $T$ , then the function  $u(t)$  will be differentiated continuously with respect to time  $t$ .

$$\frac{d^p u(t)}{dt^p} = \varphi(t, p) \text{ for all } t \in T \quad (15)$$

for  $t = t_i$ , then  $\varphi(t, p) = \varphi(t_i, p)$ , where  $p$  belongs to the set of non-negative integers, denoted as the  $p$ -domain. We can therefore write Eq. (15) as

$$U(p) = \varphi(t_i, p) = \left[ \frac{d^p u(t)}{dt^p} \right]_{t=t_i} \quad (16)$$

where  $U_p$  is called the spectrum of  $u(t)$  at

Expressing  $u(t)$  in Taylor's series as  $t = t_i$

$$u(t) = \sum_p \left[ \frac{(t-t_i)^p}{p!} \right] U(p) \quad (17)$$

where Equ. (15) is the inverse of  $U(k)$  us symbol 'D' denoting the differential transformation process and combining (16) and (17), we have

$$u(t) = \sum_{p=0}^{\infty} \left[ \frac{(t-t_i)^p}{p!} \right] U(p) = D^{-1}U(p) \quad (18)$$

### Basic concepts of multi-step differential transform method

The limitation of classical DTM is shown when is being used for solving differential equations with the boundary conditions at infinity i.e. the obtained series solution through the DTM for such equation with the boundary condition become divergent. Besides that, generally, power series solutions are not useful for large values of the independent variable. In order to overcome this shortcoming, the multi-step DTM is developed (Table 4). The basic concepts of the multi-step DTM for solving non-linear initial-value problem is presented as follows,

**Table 4** Operational properties of differential transformation method

S/N	Function	Differential transform
1	$u(t) \pm v(t)$	$U(p) \pm V(p)$
2	$\alpha u(t)$	$\alpha U(p)$
3	$\frac{du(t)}{dt}$	$(p+1)U(p+1)$
4	$u(t)v(t)$	$\sum_{r=0}^p V(r)U(p-r)$
5	$u^m(t)$	$\sum_{r=0}^p U^{m-1}(r)U(p-r)$
6	$\frac{d^n u(t)}{dx^n}$	$(p+1)(p+2)\dots(p+n)U(p+n)$
7	$\sin(\omega t + \alpha)$	$\frac{\omega^p}{p!} \sin\left(\frac{\pi p}{2!} + \alpha\right)$
8	$\cos(\omega t + \alpha)$	$Z(p) = \frac{\omega^p}{p!} \cos\left(\frac{\pi p}{2!} + \alpha\right)$

$$u(t, f, f', \dots, f^{(h)}) = 0, \quad (19)$$

subject to the initial conditions

$$f^{(k)}(0) = c_k, \quad k = 0, 1, \dots, h-1. \quad (20)$$

Let  $[0, T]$  be the interval over which we want to find the solution of the initial value problem of Eq. (19). In actual application of the DTM, the approximate solution of the initial value problem of Eq. (19) can be expressed by the following finite series:

$$f(t) = \sum_{m=0}^M a_m t^m \quad t \in [0, T] \quad (21)$$

The multi-step approach introduces a new idea for constructing the approximate solution. Assume that the interval  $[0, T]$  is divided into  $N$  subintervals  $[t_{i-1}, t_i]$ ,  $i = 1, 2, \dots, N$  of equal step size  $H = T/N$  by using the nodes  $t = iH$ . The main idea of the multi-step DTM is as follows. First, we apply the DTM to Eq. (19) over the interval  $[0, t_1]$ , we will obtain the following approximate solution,

$$f_1(t) = \sum_{m=0}^K a_{1m} t^m \quad t \in [0, t_1], \quad (22)$$

Using the initial conditions  $f^{(k)}(0) = c_k$ . For  $i \geq 2$  and at each subinterval  $[t_{i-1}, t_i]$  we will use the initial conditions  $f_i^{(k)}(t_{i-1}) = f_{i-1}^{(k)}(t_{i-1})$  and apply the DTM to Eq. (19) over the interval  $[t_{i-1}, t_i]$ , where  $t_0$  in Eq. (15) is replaced by  $t_{i-1}$ . The process

is repeated and generates a sequence of approximate solution  $f_i(t)$ ,  $i = 1, 2, \dots, N$ , for the solution  $f(t)$ ,

$$f_i(t) = \sum_{m=0}^K a_{im} (t - t_{i-1})^m, \quad t \in [t_i, t_{i+1}], \quad (23)$$

where  $M = K \cdot N$ . In fact, the multi-step DTM assumes the following solution:

$$f(t) = \begin{cases} f_1(t), & t \in [0, t_1] \\ \vdots \\ f_i(t), & t \in [t_i, t_{i+1}] \\ \vdots \\ f_N(t), & t \in [t_{N-1}, t_N] \end{cases} \quad (24)$$

which shows that there is a separate function for every sub domain.

Following the above definition, it could be stated that the multi-step DTM for every sub-domain is defined as

$$F_i(m) = \frac{H^m}{m!} \left[ \frac{d^m u(t)}{dt^m} \right]_{t=t_i} \quad (25)$$

The inverse multi-step DTM is

$$f_i(t) = \sum_{m=0}^{\infty} \left[ \frac{(t - t_i)^m}{m!} \right] F_i(m) \quad (26)$$

The new algorithm, multi-step DTM is simple for computational performance for all values of  $H$ . It is easily observed that if the step size  $H = T$ , then the multi-step DTM reduces to the classical DTM. Using the operational properties of the differential transformation method, the differential transformation of the governing differential Eq. (10) is given as

$$\begin{aligned} & (p+1)(p+2)(p+3)F(p+3) \\ & + (1-\phi)^{2.5} \left\{ \alpha_1 \left[ 3 \sum_{l=0}^p (p-l+1)(p-l+2)F(l)F(p-l+2) - 2 \sum_{l=0}^p (l+1)(p-l+1)F(l+1)F(p-l+1) \right] \right. \\ & \left. + \alpha_2 \Theta(p) \cos \gamma - (M^2 + Da^{-1})F(p) \right\} = 0 \end{aligned} \quad (27)$$

Eq. (27) can be written as

$$F(p+3) = \frac{(1-\phi)^{2.5}}{(p+1)(p+2)(p+3)} \left\{ \alpha_1 \left[ 2 \sum_{l=0}^p (l+1)(p-l+1)F(l+1)F(p-l+1) - 3 \sum_{l=0}^p (p-l+1)(p-l+2)F(l)F(p-l+2) \right] - \alpha_2 \Theta(p) \cos \gamma + (M^2 + Da^{-1})F(p) \right\} \quad (28)$$

For the Eq.(11), we have the recursive relation in differential transform domain as

$$(p+1)(p+2)\Theta(p+2) + \left\{ 3\alpha_3 Pr \sum_{l=0}^p (l+1)\Theta(l+1)F(p-l) \right\} = 0 \quad (29)$$

$$\Theta(p+2) = \frac{-3\alpha_3 Pr}{(p+1)(p+2)} \left\{ \sum_{l=0}^p (l+1)\Theta(l+1)F(p-l) \right\} \quad (30)$$

where

$$\begin{aligned} \alpha_1 &= (1-\phi) + \phi \left( \frac{\rho_s}{\rho_f} \right) \\ \alpha_2 &= \left[ (1-\phi) + \phi \left[ (\rho\beta)_s / (\rho\beta)_f \right] \right] \\ \alpha_3 &= \left[ \frac{1}{\left[ (1-\phi) + \phi \left[ (\rho C_p)_s / (\rho C_p)_f \right] \right]} \left[ \frac{k_s + (m-1)k_f - (m-1)\phi(k_f - k_s)}{k_s + (m-1)k_f + \phi(k_f - k_s)} \right] \right] \end{aligned}$$

Also, recursive relation for the boundary conditions in Eq. (13) are

$$\begin{aligned} F(p) = 0 & \Rightarrow F(0) = 0, \quad (p+1)F(p+1) = 0 \Rightarrow F(1) = 0, \quad \theta(p) = 1 \Rightarrow \theta(0) = 1, \\ F(2) &= a, \quad \theta(1) = b, \end{aligned} \quad (31)$$

where  $a$  and  $b$  are unknown constants which will be found later.

It should be noted that the transformations which included “ $a$ ” and “ $b$ ” are established from values of  $f''(0)=a$  and  $\theta'(0)=b$

From Eq. (29), we have the following boundary conditions in differential transform domain

$$F[0]=0, \quad F[1]=0, \quad \theta[0]=1, \quad F[2]=a, \quad \theta[1]=b \quad (32)$$

Using  $p=0, 1, 2, 3, 4, 5, 6, 7, \dots$  in the above recursive relations in Eq. (29), we arrived at

$$F[3] = -\frac{1}{6}(1-\phi)^{5/2} \alpha_2 \cos \gamma$$

$$F[7] = -\frac{(1-\phi)^{5/2} \alpha_2 b \cos \gamma \left( -40Da(1-\phi)^{5/2} Rd a \alpha_1 - 30(1-\phi)^{5/2} \alpha_1 a Da + 4DaM^2 Rd - 18DaPr a \alpha_3 + 3DaM^2 + 4Rd + 3 \right)}{(15120 + 20160Rd)Da}$$

$$F[8] = \frac{1}{(120960 + 161280Rd)Da^2} \left( \begin{aligned} &6a + 8Da^2M^4Rda + 16DaM^2Rda - 144(1-\phi)^{5/2} \alpha_1 a^2 Da + 312Da^2a^3\phi^5\alpha_1^2 \\ &- 1560Da^2a^3\phi^4\alpha_1^2 + 3120Da^2a^3\phi^3\alpha_1^2 - 3120Da^2a^3\phi^2\alpha_1^2 + 1560Da^2a^3\phi\alpha_1^2 \\ &- 416Da^2Rda^3\alpha_1^2 - 192Da^2M^2(1-\phi)^{5/2} Rda^2\alpha_1 - 15Da^2(1-\phi)^{5/2} b(\cos\gamma)^2\alpha_1\alpha_2^2 \\ &- 9Da^2Prb(\cos\gamma)^2\alpha_2^2\alpha_3 + 100Da^2(1-\phi)^{5/2} Rdb(\cos\gamma)^2\phi\alpha_1\alpha_2^2 \\ &- 200Da^2(1-\phi)^{5/2} Rdb(\cos\gamma)^2\phi^2\alpha_1\alpha_2^2 - 100Da^2(1-\phi)^{5/2} Rdb(\cos\gamma)^2\phi^4\alpha_1\alpha_2^2 \\ &+ 200Da^2(1-\phi)^{5/2} Rdb(\cos\gamma)^2\phi^3\alpha_1\alpha_2^2 + 20Da^2(1-\phi)^{5/2} Rdb(\cos\gamma)^2\phi^5\alpha_1\alpha_2^2 \\ &- 192Da(1-\phi)^{5/2} Rda^2\alpha_1 - 144Da^2M^2(1-\phi)^{5/2} a^2\alpha_1 - 4160Da^2Rda^3\phi^2\alpha_1^2 \\ &+ 2080Da^2Rda^3\phi\alpha_1^2 + 4160Da^2Rda^3\phi^3\alpha_1^2 + 416Da^2Rda^3\phi^5\alpha_1^2 - 2080Da^2Rda^3\phi^4\alpha_1^2 \\ &+ 8Rda + 12DaM^2a - 312Da^2a^3\alpha_1^2 + 6Da^2M^4a - 20Da^2(1-\phi)^{5/2} Rdb(\cos\gamma)^2\alpha_1\alpha_2^2 \\ &+ 75Da^2(1-\phi)^{5/2} b(\cos\gamma)^2\phi\alpha_1\alpha_2^2 + 150Da^2(1-\phi)^{5/2} b(\cos\gamma)^2\phi^3\alpha_1\alpha_2^2 \\ &- 150Da^2(1-\phi)^{5/2} b(\cos\gamma)^2\phi^2\alpha_1\alpha_2^2 + 15Da^2(1-\phi)^{5/2} b(\cos\gamma)^2\phi^5\alpha_1\alpha_2^2 \\ &- 75Da^2(1-\phi)^{5/2} b(\cos\gamma)^2\phi^4\alpha_1\alpha_2^2 + 9Da^2Prb(\cos\gamma)^2\phi^5\alpha_2^2\alpha_3 - 45Da^2Prb(\cos\gamma)^2\phi^4\alpha_2^2\alpha_3 \\ &+ 90Da^2Prb(\cos\gamma)^2\phi^3\alpha_2^2\alpha_3 - 90Da^2Prb(\cos\gamma)^2\phi^2\alpha_2^2\alpha_3 + 45Da^2Prb(\cos\gamma)^2\phi\alpha_2^2\alpha_3 \end{aligned} \right)$$

$$F[9] = -\frac{(1-\phi)^{5/2} \alpha_2 \cos \gamma}{(1088640 + 1451520Rd)Da^2} \left( \begin{aligned} &3 - 252(1-\phi)^{5/2} \alpha_1 a Da + 216Da^2a^2\phi^5\alpha_1^2 - 1080Da^2a^2\phi^4\alpha_1^2 + 2160Da^2a^2\phi^3\alpha_1^2 \\ &- 2160Da^2a^2\phi^2\alpha_1^2 + 1080Da^2a^2\phi\alpha_1^2 - 288Da^2Rda^2\alpha_1^2 - 15Da^2b^2\cos\gamma\phi^5\alpha_1\alpha_2 \\ &+ 75Da^2b^2\cos\gamma\phi^4\alpha_1\alpha_2 - 150Da^2b^2\cos\gamma\phi^3\alpha_1\alpha_2 + 150Da^2b^2\cos\gamma\phi^2\alpha_1\alpha_2 \\ &+ 20Da^2Rdb^2\cos\gamma\alpha_1\alpha_2 - 75Da^2b^2\cos\gamma\phi\alpha_1\alpha_2 - 336Da^2M^2(1-\phi)^{5/2} Rda\alpha_1 \\ &+ 8DaM^2Rd + 200Da^2Rdb^2\cos\gamma\phi^2\alpha_1\alpha_2 + 100Da^2Rdb^2\cos\gamma\phi^4\alpha_1\alpha_2 - 1440Da^2Rda^2\phi^4\alpha_1^2 \\ &- 200Da^2Rdb^2\cos\gamma\phi^3\alpha_1\alpha_2 + 9Da^2(1-\phi)^{5/2} Prb^2\cos\gamma\alpha_2\alpha_3 - 20Da^2Rdb^2\cos\gamma\phi^5\alpha_1\alpha_2 \\ &- 100Da^2Rdb^2\cos\gamma\phi\alpha_1\alpha_2 - 336Da(1-\phi)^{5/2} Rda\alpha_1 + 288Da^2Rda^2\phi^5\alpha_1^2 \\ &+ 15Da^2b^2\cos\gamma\alpha_1\alpha_2 - 252Da^2M^2(1-\phi)^{5/2} a\alpha_1 - 2880Da^2Rda^2\phi^2\alpha_1^2 + 1440Da^2Rda^2\phi\alpha_1^2 \\ &+ 2880Da^2Rda^2\phi^3\alpha_1^2 + 6M^2Da + 3Da^2M^4 + 4Da^2M^4Rd - 216Da^2a^2\alpha_1^2 + 4Rd \end{aligned} \right)$$

$$F[10] = -\frac{(1-\phi)^{5/2} \alpha_2 \cos \gamma}{3628800(3+4Rd)^2 Da^2} \left( \begin{aligned} &-77760 Da^2 Rd a^2 b \phi \alpha_1^2 + 9b + 5832 Da^2 a^2 b \alpha_1^2 + 16 Da^2 M^4 Rd^2 b + 24 Da^2 M^4 Rd b \\ &+ 32 Da M^2 Rd^2 b + 48 Da M^2 Rd b + 378 Da \cos \gamma \alpha_1 \alpha_2 - 378 Da^2 M^2 \cos \gamma \phi^5 \alpha_1 \alpha_2 \\ &+ 1890 Da^2 M^2 \cos \gamma \phi^4 \alpha_1 \alpha_2 - 672 Da Rd^2 \cos \gamma \phi^5 \alpha_1 \alpha_2 - 3780 Da^2 M^2 \cos \gamma \phi^3 \alpha_1 \alpha_2 \\ &+ 3360 Da Rd^2 \cos \gamma \phi^4 \alpha_1 \alpha_2 - 1008 Da Rd \cos \gamma \phi^5 \alpha_1 \alpha_2 + 672 Da^2 M^2 Rd^2 \cos \gamma \alpha_1 \alpha_2 \\ &- 6720 Da Rd^2 \cos \gamma \phi^3 \alpha_1 \alpha_2 + 5040 Da Rd \cos \gamma \phi^4 \alpha_1 \alpha_2 - 10368 Da^2 Rd^2 a^2 b \phi^5 \alpha_1^2 \\ &+ 51840 Da^2 Rd^2 a^2 b \phi^4 \alpha_1^2 - 15552 Da^2 Rd a^2 b \phi^5 \alpha_1^2 - 103680 Da^2 Rd^2 a^2 b \phi^3 \alpha_1^2 \\ &+ 77760 Da^2 Rd a^2 b \phi^4 \alpha_1^2 + 103680 Da^2 Rd^2 a^2 b \phi^2 \alpha_1^2 - 155520 Da^2 Rd a^2 b \phi^3 \alpha_1^2 \\ &- 51840 Da^2 Rd^2 a^2 b \phi \alpha_1^2 + 155520 Da^2 Rd a^2 b \phi^2 \alpha_1^2 + 5328 Da^2 (1-\phi)^{5/2} Pr Rd a^2 b \alpha_1 \alpha_3 \\ &+ 3780 Da \cos \gamma \phi^2 \alpha_1 \alpha_2 + 672 Da Rd^2 \cos \gamma \alpha_1 \alpha_2 + 378 Da^2 M^2 \cos \gamma \alpha_1 \alpha_2 + 3360 Da^2 M^2 Rd^2 \cos \gamma \phi^4 \alpha_1 \alpha_2 \\ &- 3780 Da \cos \gamma \phi^3 \alpha_1 \alpha_2 + 1890 Da \cos \gamma \phi^4 \alpha_1 \alpha_2 + 3240 Da^2 Pr a^2 b \alpha_3^2 - 378 Da \cos \gamma \phi^5 \alpha_1 \alpha_2 \\ &+ 10080 Da^2 M^2 Rd \cos \gamma \phi^2 \alpha_1 \alpha_2 - 3360 Da^2 M^2 Rd^2 \cos \gamma \phi \alpha_1 \alpha_2 - 10080 Da^2 M^2 Rd \cos \gamma \phi^3 \alpha_1 \alpha_2 \\ &+ 6720 Da^2 M^2 Rd^2 \cos \gamma \phi^2 \alpha_1 \alpha_2 + 5040 Da^2 M^2 Rd \cos \gamma \phi^4 \alpha_1 \alpha_2 - 6720 Da^2 M^2 Rd^2 \cos \gamma \phi^3 \alpha_1 \alpha_2 \\ &- 1008 Da^2 M^2 Rd \cos \gamma \phi^5 \alpha_1 \alpha_2 - 3408 Da (1-\phi)^{5/2} Rd a b \alpha_1 + 3780 Da^2 M^2 \cos \gamma \phi^2 \alpha_1 \alpha_2 \\ &- 2272 Da (1-\phi)^{5/2} Rd^2 a b \alpha_1 - 1278 Da^2 M^2 (1-\phi)^{5/2} a b \alpha_1 - 5040 Da Rd \cos \gamma \phi \alpha_1 \alpha_2 \\ &- 144 Da Pr Rd a b \alpha_3 + 10080 Da Rd \cos \gamma \phi^2 \alpha_1 \alpha_2 - 3360 Da Rd^2 \cos \gamma \phi \alpha_1 \alpha_2 - 10080 Da Rd \cos \gamma \phi^3 \alpha_1 \alpha_2 \\ &+ 6720 Da Rd^2 \cos \gamma \phi^2 \alpha_1 \alpha_2 - 1890 Da^2 M^2 \cos \gamma \phi \alpha_1 \alpha_2 + 1008 Da^2 M^2 Rd \cos \gamma \alpha_1 \alpha_2 \\ &- 672 Da^2 M^2 Rd^2 \cos \gamma \phi^5 \alpha_1 \alpha_2 - 108 Da^2 M^2 Pr a b \alpha_3 + 9 Da^2 M^4 b + 18 Da M^2 b - 1278 Da (1-\phi)^{5/2} a b \alpha_1 \\ &- 108 Da Pr a b \alpha_3 + 1008 Da Rd \cos \gamma \alpha_1 \alpha_2 - 1890 Da \cos \gamma \phi \alpha_1 \alpha_2 + 58320 Da^2 a^2 b \phi^2 \alpha_1^2 - 29160 Da^2 a^2 b \phi \alpha_1^2 \\ &+ 29160 Da^2 a^2 b \phi^4 \alpha_1^2 - 58320 Da^2 a^2 b \phi^3 \alpha_1^2 - 5832 Da^2 a^2 b \phi^5 \alpha_1^2 + 10368 Da^2 Rd^2 a^2 b \alpha_1^2 \\ &+ 15552 Da^2 Rd a^2 b \alpha_1^2 + 16 Rd^2 b + 24 Rd b - 5040 Da^2 M^2 Rd \cos \gamma \phi \alpha_1 \alpha_2 - 144 Da^2 M^2 Pr Rd a b \alpha_3 \\ &+ 3996 Da^2 (1-\phi)^{5/2} Pr a^2 b \alpha_1 \alpha_3 - 3408 Da^2 M^2 (1-\phi)^{5/2} Rd a b \alpha_1 - 2272 Da^2 M^2 (1-\phi)^{5/2} Rd^2 a b \alpha_1 \end{aligned} \right)$$

In the same manner, the expressions for  $F[11]$ ,  $F[12]$ ,  $F[13]$ ,  $F[14]$ ,  $F[15]$  are found but they are too large to be included in this paper.

Also, using  $p=0, 1, 2, 3 \dots$  in the above recursive relations in Eq. (30), we arrived at following solutions

$$\begin{aligned} \Theta[2] &= 0 \\ \Theta[3] &= 0 \\ \Theta[4] &= -\frac{3}{4} \left( \frac{\alpha_3 Pr a b}{3+4Rd} \right) \\ \Theta[5] &= \frac{3\alpha_3 Pr (1-\phi)^{5/2} b \alpha_2 \cos \gamma}{120+160Rd} \\ \Theta[6] &= \frac{\alpha_3 Pr b^2 (1-\phi)^{5/2} \alpha_2 \cos \gamma}{240+320Rd} \\ \Theta[7] &= -\frac{\alpha_3 Pr b a \left( 3+8Da(1-\phi)^{5/2} Rd a \alpha_1 + 6(1-\phi)^{5/2} \alpha_1 a Da + 4DaM^2Rd - 180DaPra\alpha_3 + 3DaM^2 + 4Rd \right)}{280(3+4Rd)^2 Da} \\ \Theta[8] &= \frac{\alpha_3 Pr (1-\phi)^{5/2} b \alpha_2 \cos \gamma (4DaM^2Rd - 630DaPra\alpha_3 + 3DaM^2 + 4Rd + 3)}{4480(3+4Rd)^2 Da} \\ \Theta[9] &= \frac{\alpha_3 Pr b \alpha_2 \cos \gamma}{40320(3+4Rd)^2 Da} \left( \begin{aligned} &4DaM^2(1-\phi)^{5/2} Rd b - 1026\alpha_3 Pr b a (1-\phi)^{5/2} Da - 315 Da Pr \cos \gamma \phi^5 \alpha_2 \alpha_3 \\ &+ 40 Da Rd a b \phi^5 \alpha_1 + 3 Da M^2 (1-\phi)^{5/2} b + 1575 Da Pr \cos \gamma \phi^4 \alpha_2 \alpha_3 \\ &- 200 Da Rd a b \phi^4 \alpha_1 + 30 Da a b \phi^5 \alpha_1 + 150 Da a b \phi \alpha_1 - 30 Da a b \alpha_1 \\ &- 3150 Da Pr \cos \gamma \phi^3 \alpha_2 \alpha_3 + 400 Da Rd a b \phi^3 \alpha_1 - 150 Da a b \phi^4 \alpha_1 \\ &+ 3150 Da Pr \cos \gamma \phi^2 \alpha_2 \alpha_3 - 400 Da Rd a b \phi^2 \alpha_1 + 300 Da a b \phi^3 \alpha_1 \\ &+ 4(1-\phi)^{5/2} Rd b - 1575 Da Pr \cos \gamma \phi \alpha_2 \alpha_3 + 200 Da Rd a b \phi \alpha_1 \\ &- 300 Da a b \phi^2 \alpha_1 + 3b(1-\phi)^{5/2} + 315\alpha_3 Pr \alpha_2 \cos \gamma Da - 40 Da Rd a b \alpha_1 \end{aligned} \right) \end{aligned}$$

$$\Theta[10] = -\frac{\alpha_3 \text{Pr} b}{403200(3+4Rd)^3 Da^2} \left( \begin{aligned} &-1152 Da^2 M^2 (1-\phi)^{5/2} Rd a^2 \alpha_1 - 450 Da^2 (1-\phi)^{5/2} b(\cos\gamma)^2 \phi^2 \alpha_1 \alpha_2^2 + 18a - 9072 \alpha_3 \text{Pr} a^2 Da \\ &+ 48 Da^2 M^4 Rd a + 96 Da M^2 Rd a - 432 (1-\phi)^{5/2} \alpha_1 a^2 Da + 936 Da^2 a^3 \phi^5 \alpha_1^2 - 4680 Da^2 a^3 \phi^4 \alpha_1^2 \\ &+ 9360 Da^2 a^3 \phi^3 \alpha_1^2 - 9360 Da^2 a^3 \phi^2 \alpha_1^2 + 4680 Da^2 a^3 \phi \alpha_1^2 - 45 Da^2 (1-\phi)^{5/2} b(\cos\gamma)^2 \alpha_1 \alpha_2^2 \\ &- 12096 Da^2 M^2 \text{Pr} Rd a^2 \alpha_3 - 18144 Da^2 (1-\phi)^{5/2} \text{Pr} a^3 \alpha_1 \alpha_3 - 768 Da^2 M^2 (1-\phi)^{5/2} Rd^2 a^2 \alpha_1 \\ &- 12096 Da \text{Pr} Rd a^2 \alpha_3 - 9072 Da^2 M^2 \text{Pr} a^2 \alpha_3 + 450 Da^2 (1-\phi)^{5/2} b(\cos\gamma)^2 \phi^3 \alpha_1 \alpha_2^2 \\ &- 225 Da^2 (1-\phi)^{5/2} b(\cos\gamma)^2 \phi^4 \alpha_1 \alpha_2^2 + 45 Da^2 (1-\phi)^{5/2} b(\cos\gamma)^2 \phi^5 \alpha_1 \alpha_2^2 + 3429 Da^2 \text{Pr} b(\cos\gamma)^2 \phi^5 \alpha_2^2 \alpha_3 \\ &+ 34290 Da^2 \text{Pr} b(\cos\gamma)^2 \phi^3 \alpha_2^2 \alpha_3 - 34290 Da^2 \text{Pr} b(\cos\gamma)^2 \phi^2 \alpha_2^2 \alpha_3 - 80 Da^2 (1-\phi)^{5/2} Rd^2 b(\cos\gamma)^2 \alpha_1 \alpha_2^2 \\ &- 4572 Da^2 \text{Pr} Rd b(\cos\gamma)^2 \alpha_2^2 \alpha_3 - 17145 Da^2 \text{Pr} b(\cos\gamma)^2 \phi^4 \alpha_2^2 \alpha_3 - 120 Da^2 (1-\phi)^{5/2} Rd b(\cos\gamma)^2 \alpha_1 \alpha_2^2 \\ &- 24192 Da^2 (1-\phi)^{5/2} \text{Pr} Rd a^3 \alpha_1 \alpha_3 + 225 Da^2 (1-\phi)^{5/2} b(\cos\gamma)^2 \phi \alpha_1 \alpha_2^2 + 600 Da^2 (1-\phi)^{5/2} Rd b(\cos\gamma)^2 \phi \alpha_1 \alpha_2^2 \\ &- 1200 Da^2 (1-\phi)^{5/2} Rd b(\cos\gamma)^2 \phi^2 \alpha_1 \alpha_2^2 + 1200 Da^2 (1-\phi)^{5/2} Rd b(\cos\gamma)^2 \phi^3 \alpha_1 \alpha_2^2 \\ &- 600 Da^2 (1-\phi)^{5/2} Rd b(\cos\gamma)^2 \phi^4 \alpha_1 \alpha_2^2 + 120 Da^2 (1-\phi)^{5/2} Rd b(\cos\gamma)^2 \phi^5 \alpha_1 \alpha_2^2 + 32 Rd^2 a \\ &+ 18 Da^2 M^4 a - 1152 Da (1-\phi)^{5/2} Rd a^2 \alpha_1 - 432 Da^2 M^2 (1-\phi)^{5/2} a^2 \alpha_1 + 12480 Da^2 Rd a^3 \phi \alpha_1^2 \\ &- 936 Da^2 a^3 \alpha_1^2 - 3429 Da^2 \text{Pr} b(\cos\gamma)^2 \alpha_2^2 \alpha_3 + 17145 Da^2 \text{Pr} b(\cos\gamma)^2 \phi \alpha_2^2 \alpha_3 \\ &+ 400 Da^2 (1-\phi)^{5/2} Rd^2 b(\cos\gamma)^2 \phi \alpha_1 \alpha_2^2 + 36 Da M^2 a + 800 Da^2 (1-\phi)^{5/2} Rd^2 b(\cos\gamma)^2 \phi^3 \alpha_1 \alpha_2^2 \\ &- 800 Da^2 (1-\phi)^{5/2} Rd^2 b(\cos\gamma)^2 \phi^2 \alpha_1 \alpha_2^2 + 80 Da^2 (1-\phi)^{5/2} Rd^2 b(\cos\gamma)^2 \phi^5 \alpha_1 \alpha_2^2 - 400 Da^2 (1-\phi)^{5/2} Rd^2 b(\cos\gamma)^2 \phi^4 \alpha_1 \alpha_2^2 \\ &- 45720 Da^2 \text{Pr} Rd b(\cos\gamma)^2 \phi^2 \alpha_2^2 \alpha_3 + 22860 Da^2 \text{Pr} Rd b(\cos\gamma)^2 \phi \alpha_2^2 \alpha_3 + 4572 Da^2 \text{Pr} Rd b(\cos\gamma)^2 \phi^5 \alpha_2^2 \alpha_3 \\ &- 22860 Da^2 \text{Pr} Rd b(\cos\gamma)^2 \phi^4 \alpha_2^2 \alpha_3 + 45720 Da^2 \text{Pr} Rd b(\cos\gamma)^2 \phi^3 \alpha_2^2 \alpha_3 - 24960 Da^2 Rd a^3 \phi^3 \alpha_1^2 + 24960 Da^2 Rd a^3 \phi^3 \alpha_1^2 \\ &- 12480 Da^2 Rd a^3 \phi^4 \alpha_1^2 + 2496 Da^2 Rd a^3 \phi^5 \alpha_1^2 + 8320 Da^2 Rd^2 a^3 \phi \alpha_1^2 + 181440 Da^2 \text{Pr} a^3 \alpha_3^2 + 48 Rd a \\ &+ 16640 Da^2 Rd^2 a^3 \phi^3 \alpha_1^2 - 16640 Da^2 Rd^2 a^3 \phi^2 \alpha_1^2 - 8320 Da^2 Rd^2 a^3 \phi^4 \alpha_1^2 - 768 Da (1-\phi)^{5/2} Rd^2 a^2 \alpha_1 \\ &+ 1664 Da^2 Rd^2 a^3 \phi^5 \alpha_1^2 - 2496 Da^2 Rd a^3 \alpha_1^2 + 64 Da M^2 Rd^2 a + 32 Da^2 M^4 Rd^2 a - 1664 Da^2 Rd^2 a^3 \alpha_1^2 \end{aligned} \right)$$

In the same manner, the expressions for  $\Theta[11]$ ,  $\Theta[12]$ ,  $\Theta[13]$ ,  $\Theta[13]$ ,  $\Theta[15]$ ... are found but they are too large to be included in this paper

From the definition in Eq. (18), the solutions of Eqs. (10) and (11) are given as

$$f(\eta) = F[0] + \eta F[1] + \eta^2 F[2] + \eta^3 F[3] + \eta^4 F[4] + \eta^5 F[5] + \eta^6 F[6] + \eta^7 F[7] + \eta^8 F[8] + \eta^9 F[9] + \eta^{10} F[10] + \dots \quad (33)$$

$$\theta(\eta) = \Theta[0] + \eta \Theta[1] + \eta^2 \Theta[2] + \eta^3 \Theta[3] + \eta^4 \Theta[4] + \eta^5 \Theta[5] + \eta^6 \Theta[6] + \eta^7 \Theta[7] + \eta^8 \Theta[8] + \eta^9 \Theta[9] + \eta^{10} \Theta[10] + \dots \quad (34)$$

Now, consider similar fully coupled third and second orders ordinary differential equations presented in Eqs. (11) and (12), but at this time, we take  $a=1$  and  $b=1$

$$g''(\eta) + (1-\phi)^{2.5} \left\{ \alpha_1 \left( 3g(\eta)g''(\eta) - 2(f'(\eta))^2 \right) + \alpha_2 \mathcal{G}(\eta) \cos\gamma - (M^2 + Da^{-1})g(\eta) \right\} = 0 \quad (35)$$

$$\mathcal{G}''(\eta) + 3\alpha_3 \text{Pr} g(\eta) \mathcal{G}'(\eta) = 0 \quad (36)$$

With initial conditions as

$$g = 0, \quad g' = 0, \quad g'' = 1, \quad \mathcal{G} = 1, \quad \mathcal{G}' = 1 \quad \text{when } \eta = 0 \quad (37)$$

Following the similar solution procedures of Eqs. (10) and (11), the solutions of Eqs. (35) and (36) are

$$g(\eta) = G[0] + \eta G[1] + \eta^2 G[2] + \eta^3 G[3] + \eta^4 G[4] + \eta^5 G[5] + \eta^6 G[6] + \eta^7 G[7] + \eta^8 G[8] + \eta^9 G[9] + \eta^{10} G[10] + \dots \quad (38)$$

$$\mathcal{G}(\eta) = \Phi[0] + \eta \Phi[1] + \eta^2 \Phi[2] + \eta^3 \Phi[3] + \eta^4 \Phi[4] + \eta^5 \Phi[5] + \eta^6 \Phi[6] + \eta^7 \Phi[7] + \eta^8 \Phi[8] + \eta^9 \Phi[9] + \eta^{10} \Phi[10] + \dots \quad (39)$$

where

$$G[7] = -\frac{(1-\phi)^{5/2} \alpha_2 \cos\gamma \left( -20 Da (1-\phi)^{5/2} Rd \alpha_1 - 15 (1-\phi)^{5/2} \alpha_1 Da + 4 Da M^2 Rd - 9 Da \text{Pr} \alpha_3 + 3 Da M^2 + 4 Rd + 3 \right)}{(15120 + 20160 Rd) Da}$$

$$G[0] = 0, \quad G[1] = 0, \quad G[2] = \frac{1}{2}, \quad \theta[0] = 1, \quad \theta[1] = 1$$

$$G[3] = -\frac{1}{6} (1-\phi)^{5/2} \alpha_2 \cos\gamma$$

$$G[4] = -\frac{1}{24} (1-\phi)^{5/2} \alpha_2 \cos\gamma$$

$$G[5] = \frac{\left( (1-\phi)^{5/2} \alpha_1 Da + M^2 Da + 1 \right)}{120 Da}$$

$$G[6] = -\frac{(Da M^2 + 1)(1-\phi)^{5/2} \alpha_2 \cos\gamma}{720 Da}$$

$$\begin{aligned}
 G[8] &= \frac{1}{(120960 + 161280Rd)Da^2} \left( \begin{aligned}
 &3 + 4Da^2M^4Rd + 8DaM^2Rd - 36(1-\phi)^{5/2}\alpha_1Da + 78Da^2a^3\phi^5\alpha_1^2 \\
 &-195Da^2\phi^4\alpha_1^2 + 390Da^2\phi^3\alpha_1^2 - 390Da^2\phi^2\alpha_1^2 + 195Da^2\phi\alpha_1^2 \\
 &-52Da^2Rd\alpha_1^2 - 48Da^2M^2(1-\phi)^{5/2}Rd\alpha_1 - 15Da^2(1-\phi)^{5/2}(\cos\gamma)^2\alpha_1\alpha_2^2 \\
 &-9Da^2Pr(\cos\gamma)^2\alpha_2^2\alpha_3 + 100Da^2(1-\phi)^{5/2}Rd(\cos\gamma)^2\phi\alpha_1\alpha_2^2 \\
 &-200Da^2(1-\phi)^{5/2}Rd(\cos\gamma)^2\phi^2\alpha_1\alpha_2^2 - 100Da^2(1-\phi)^{5/2}Rd(\cos\gamma)^2\phi^4\alpha_1\alpha_2^2 \\
 &+200Da^2(1-\phi)^{5/2}Rd(\cos\gamma)^2\phi^3\alpha_1\alpha_2^2 + 20Da^2(1-\phi)^{5/2}Rd(\cos\gamma)^2\phi^5\alpha_1\alpha_2^2 \\
 &-48Da(1-\phi)^{5/2}Rd\alpha_1 - 36Da^2M^2(1-\phi)^{5/2}\alpha_1 - 520Da^2Rd\phi^2\alpha_1^2 \\
 &+260Da^2Rd\phi\alpha_1^2 + 520Da^2Rd\phi^3\alpha_1^2 + 52Da^2Rd\phi^5\alpha_1^2 - 260Da^2Rd\phi^4\alpha_1^2 \\
 &+4Rd + 6DaM^2 - 39Da^2\alpha_1^2 + 3Da^2M^4 - 20Da^2(1-\phi)^{5/2}Rd(\cos\gamma)^2\alpha_1\alpha_2^2 \\
 &+75Da^2(1-\phi)^{5/2}(\cos\gamma)^2\phi\alpha_1\alpha_2^2 + 150Da^2(1-\phi)^{5/2}(\cos\gamma)^2\phi^3\alpha_1\alpha_2^2 \\
 &-150Da^2(1-\phi)^{5/2}(\cos\gamma)^2\phi^2\alpha_1\alpha_2^2 + 15Da^2(1-\phi)^{5/2}(\cos\gamma)^2\phi^5\alpha_1\alpha_2^2 \\
 &-75Da^2(1-\phi)^{5/2}(\cos\gamma)^2\phi^4\alpha_1\alpha_2^2 + 9Da^2Pr(\cos\gamma)^2\phi^5\alpha_2^2\alpha_3 - 45Da^2Pr(\cos\gamma)^2\phi^4\alpha_2^2\alpha_3 \\
 &+90Da^2Pr(\cos\gamma)^2\phi^3\alpha_2^2\alpha_3 - 90Da^2Pr(\cos\gamma)^2\phi^2\alpha_2^2\alpha_3 + 45Da^2Pr(\cos\gamma)^2\phi\alpha_2^2\alpha_3
 \end{aligned} \right) \\
 G[9] &= -\frac{(1-\phi)^{5/2}\alpha_2\cos\gamma}{(1088640 + 1451520Rd)Da^2} \left( \begin{aligned}
 &3 - 126(1-\phi)^{5/2}\alpha_1Da + 54Da^2\phi^5\alpha_1^2 - 270Da^2\phi^4\alpha_1^2 + 540Da^2\phi^3\alpha_1^2 \\
 &-540Da^2\phi^2\alpha_1^2 + 270Da^2\phi\alpha_1^2 - 72Da^2Rd\alpha_1^2 - 15Da^2\cos\gamma\phi^5\alpha_1\alpha_2 \\
 &+75Da^2\cos\gamma\phi^4\alpha_1\alpha_2 - 150Da^2\cos\gamma\phi^3\alpha_1\alpha_2 + 150Da^2\cos\gamma\phi^2\alpha_1\alpha_2 \\
 &+20Da^2Rd\cos\gamma\alpha_1\alpha_2 - 75Da^2\cos\gamma\phi\alpha_1\alpha_2 - 168Da^2M^2(1-\phi)^{5/2}Rda_1 \\
 &+4DaM^2Rd + 200Da^2Rd\cos\gamma\phi^2\alpha_1\alpha_2 + 100Da^2Rd\cos\gamma\phi^4\alpha_1\alpha_2 - 360Da^2Rd\phi^4\alpha_1^2 \\
 &-200Da^2Rd\cos\gamma\phi^3\alpha_1\alpha_2 + 9Da^2(1-\phi)^{5/2}Pr\cos\gamma\alpha_2\alpha_3 - 20Da^2Rd\cos\gamma\phi^5\alpha_1\alpha_2 \\
 &-100Da^2Rd\cos\gamma\phi\alpha_1\alpha_2 - 168Da(1-\phi)^{5/2}Rda_1 + 72Da^2Rd\phi^5\alpha_1^2 \\
 &+15Da^2\cos\gamma\alpha_1\alpha_2 - 126Da^2M^2(1-\phi)^{5/2}\alpha_1 - 720Da^2Rd\phi^2\alpha_1^2 + 360Da^2Rd\phi^2\alpha_1^2 \\
 &+720Da^2Rd\phi^3\alpha_1^2 + 6M^2Da + 3Da^2M^4 + 4Da^2M^4Rd - 54Da^2\alpha_1^2 + 4Rd
 \end{aligned} \right) \\
 G[10] &= -\frac{(1-\phi)^{5/2}\alpha_2\cos\gamma}{3628800(3+4Rd)^2Da^2} \left( \begin{aligned}
 &-19440Da^2Rd\phi\alpha_1^2 + 9b + 1458Da^2\alpha_1^2 + 16Da^2M^4Rd^2 + 24Da^2M^4Rd \\
 &+32DaM^2Rd^2 + 48DaM^2Rd + 378Da\cos\gamma\alpha_1\alpha_2 - 378Da^2M^2\cos\gamma\phi^5\alpha_1\alpha_2 \\
 &+1890Da^2M^2\cos\gamma\phi^4\alpha_1\alpha_2 - 672DaRd^2\cos\gamma\phi^5\alpha_1\alpha_2 - 3780Da^2M^2\cos\gamma\phi^3\alpha_1\alpha_2 \\
 &+3360DaRd^2\cos\gamma\phi^4\alpha_1\alpha_2 - 1008DaRd\cos\gamma\phi^5\alpha_1\alpha_2 + 672Da^2M^2Rd^2\cos\gamma\alpha_1\alpha_2 \\
 &-6720DaRd^2\cos\gamma\phi^3\alpha_1\alpha_2 + 5040DaRd\cos\gamma\phi^4\alpha_1\alpha_2 - 2592Da^2Rd^2\phi^5\alpha_1^2 \\
 &+12960Da^2Rd^2\phi^4\alpha_1^2 - 3888Da^2Rd\phi^5\alpha_1^2 - 25920Da^2Rd^2\phi^3\alpha_1^2 \\
 &+77760Da^2Rda^2\phi^4\alpha_1^2 + 25920Da^2Rd^2\alpha_1^2 - 77760Da^2Rda^2\alpha_1^2 \\
 &-12960Da^2Rd^2\phi\alpha_1^2 + 38880Da^2Rd\phi^2\alpha_1^2 + 1332Da^2(1-\phi)^{5/2}PrRd\alpha_1\alpha_3 \\
 &+3780Da\cos\gamma\phi^2\alpha_1\alpha_2 + 672DaRd^2\cos\gamma\alpha_1\alpha_2 + 378Da^2M^2\cos\gamma\alpha_1\alpha_2 + 3360Da^2M^2Rd^2\cos\gamma\phi^4\alpha_1\alpha_2 \\
 &-3780Da\cos\gamma\phi^3\alpha_1\alpha_2 + 1890Da\cos\gamma\phi^4\alpha_1\alpha_2 + 810Da^2Prb\alpha_3^2 - 378Da\cos\gamma\phi^5\alpha_1\alpha_2 \\
 &+10080Da^2M^2Rd\cos\gamma\phi^2\alpha_1\alpha_2 - 3360Da^2M^2Rd^2\cos\gamma\phi\alpha_1\alpha_2 - 10080Da^2M^2Rd\cos\gamma\phi^3\alpha_1\alpha_2 \\
 &+6720Da^2M^2Rd^2\cos\gamma\phi^2\alpha_1\alpha_2 + 5040Da^2M^2Rd\cos\gamma\phi^4\alpha_1\alpha_2 - 6720Da^2M^2Rd^2\cos\gamma\phi^3\alpha_1\alpha_2 \\
 &-1008Da^2M^2Rd\cos\gamma\phi^5\alpha_1\alpha_2 - 1704Da(1-\phi)^{5/2}Rd\alpha_1 + 3780Da^2M^2\cos\gamma\phi^2\alpha_1\alpha_2 \\
 &-1138Da(1-\phi)^{5/2}Rd^2\alpha_1 - 639Da^2M^2(1-\phi)^{5/2}\alpha_1 - 5040DaRd\cos\gamma\phi\alpha_1\alpha_2 \\
 &-72DaPrRd\alpha_3 + 10080DaRd\cos\gamma\phi^2\alpha_1\alpha_2 - 3360DaRd^2\cos\gamma\phi\alpha_1\alpha_2 - 10080DaRd\cos\gamma\phi^3\alpha_1\alpha_2 \\
 &+6720DaRd^2\cos\gamma\phi^2\alpha_1\alpha_2 - 1890Da^2M^2\cos\gamma\phi\alpha_1\alpha_2 + 1008Da^2M^2Rd\cos\gamma\alpha_1\alpha_2 \\
 &-672Da^2M^2Rd^2\cos\gamma\phi^5\alpha_1\alpha_2 - 54Da^2M^2Pr\alpha_3 + 9Da^2M^4 + 18DaM^2 - 639Da(1-\phi)^{5/2}\alpha_1 \\
 &-54DaPr\alpha_3 + 1008DaRd\cos\gamma\alpha_1\alpha_2 - 1890Da\cos\gamma\phi\alpha_1\alpha_2 + 14580Da^2b\phi^2\alpha_1^2 - 7290Da^2\phi\alpha_1^2 \\
 &+7290Da^2\phi^4\alpha_1^2 - 14580Da^2b\phi^3\alpha_1^2 - 1458Da^2\phi^5\alpha_1^2 + 2592Da^2Rd^2\alpha_1^2 \\
 &+3888Da^2Rd\alpha_1^2 + 16Rd^2 + 24Rd - 5040Da^2M^2Rd\cos\gamma\phi\alpha_1\alpha_2 - 72Da^2M^2PrRd\alpha_3 \\
 &+999Da^2(1-\phi)^{5/2}Pr\alpha_1\alpha_3 - 1704Da^2M^2(1-\phi)^{5/2}Rd\alpha_1 - 1388Da^2M^2(1-\phi)^{5/2}Rd^2\alpha_1
 \end{aligned} \right)
 \end{aligned}$$

Similarly

$$\begin{aligned}
 \Phi[2] &= 0 \\
 \Phi[3] &= 0 \\
 \Phi[4] &= -\frac{3}{8} \left( \frac{\alpha_3 \text{Pr}}{3+4Rd} \right) \\
 \Phi[5] &= \frac{3\alpha_3 \text{Pr}(1-\phi)^{5/2} \alpha_2 \cos\gamma}{120+160Rd} \\
 \Phi[6] &= \frac{\alpha_3 \text{Pr}(1-\phi)^{5/2} \alpha_2 \cos\gamma}{240+320Rd} \\
 \Phi[7] &= -\frac{\alpha_3 \text{Pr} \left( 3+4Da(1-\phi)^{5/2} Rd \alpha_1 + 3(1-\phi)^{5/2} \alpha_1 Da \right.}{4DaM^2 Rd - 90Da \text{Pr} \alpha_3 + 3DaM^2 + 4Rd} \\
 &\quad \left. + 4Rd \right) / 560(3+4Rd)^2 Da \\
 \Phi[8] &= \frac{\alpha_3 \text{Pr}(1-\phi)^{5/2} \alpha_2 \cos\gamma (4DaM^2 Rd - 315Da \text{Pr} \alpha_3 + 3DaM^2 + 4Rd + 3)}{4480(3+4Rd)^2 Da} \\
 \Phi[9] &= \frac{\alpha_3 \text{Pr} \alpha_2 \cos\gamma}{40320(3+4Rd)^2 Da} \left( \begin{aligned} &4DaM^2(1-\phi)^{5/2} Rd - 516\alpha_3 \text{Pr} b(1-\phi)^{5/2} Da - 315Da \text{Pr} \cos\gamma \phi^5 \alpha_2 \alpha_3 \\ &+ 20Da Rd \phi^5 \alpha_1 + 3DaM^2(1-\phi)^{5/2} + 1575Da \text{Pr} \cos\gamma \phi^4 \alpha_2 \alpha_3 \\ &- 100Da Rd \phi^4 \alpha_1 + 15Da \phi^5 \alpha_1 + 75Da \phi \alpha_1 - 15Da \alpha_1 \\ &- 3150Da \text{Pr} \cos\gamma \phi^3 \alpha_2 \alpha_3 + 200Da Rd \phi^3 \alpha_1 - 75Da \phi^4 \alpha_1 \\ &+ 3150Da \text{Pr} \cos\gamma \phi^2 \alpha_2 \alpha_3 - 200Da Rd \phi^2 \alpha_1 + 150Da \phi^3 \alpha_1 \\ &+ 4(1-\phi)^{5/2} Rd - 1575Da \text{Pr} \cos\gamma \phi \alpha_2 \alpha_3 + 100Da Rd \phi \alpha_1 \\ &- 150Da \phi^2 \alpha_1 + 3(1-\phi)^{5/2} + 315\alpha_3 \text{Pr} \alpha_2 \cos\gamma Da - 20Da Rd \alpha_1 \end{aligned} \right) \\
 \Phi[10] &= -\frac{\alpha_3 \text{Pr} b}{403200(3+4Rd)^3 Da^2} \left( \begin{aligned} &-1152Da^2 M^2 (1-\phi)^{5/2} Rd a^2 \alpha_1 - 450Da^2 (1-\phi)^{5/2} (\cos\gamma)^2 \phi^2 \alpha_1 \alpha_2^2 + 9 - 2268\alpha_3 \text{Pr} Da \\ &+ 24Da^2 M^4 Rd + 48DaM^2 Rd - 108(1-\phi)^{5/2} \alpha_1 Da + 117Da^2 \phi^5 \alpha_1^2 - 585Da^2 \phi^4 \alpha_1^2 \\ &+ 1170Da^2 \phi^3 \alpha_1^2 - 1170Da^2 \phi^2 \alpha_1^2 + 585Da^2 \phi \alpha_1^2 - 45Da^2 (1-\phi)^{5/2} (\cos\gamma)^2 \alpha_1 \alpha_2^2 \\ &- 3024Da^2 M^2 \text{Pr} Rd \alpha_3 - 2268Da^2 (1-\phi)^{5/2} \text{Pr} \alpha_1 \alpha_3 - 192Da^2 M^2 (1-\phi)^{5/2} Rd^2 \alpha_1 \\ &- 3024Da \text{Pr} Rd \alpha_3 - 2268Da^2 M^2 \text{Pr} \alpha_3 + 450Da^2 (1-\phi)^{5/2} (\cos\gamma)^2 \phi^3 \alpha_1 \alpha_2^2 \\ &- 225Da^2 (1-\phi)^{5/2} (\cos\gamma)^2 \phi^4 \alpha_1 \alpha_2^2 + 45Da^2 (1-\phi)^{5/2} (\cos\gamma)^2 \phi^5 \alpha_1 \alpha_2^2 + 3429Da^2 \text{Pr} (\cos\gamma)^2 \phi^5 \alpha_2^2 \alpha_3 \\ &+ 34290Da^2 \text{Pr} (\cos\gamma)^2 \phi^3 \alpha_2^2 \alpha_3 - 34290Da^2 \text{Pr} (\cos\gamma)^2 \phi^2 \alpha_2^2 \alpha_3 - 80Da^2 (1-\phi)^{5/2} Rd^2 (\cos\gamma)^2 \alpha_1 \alpha_2^2 \\ &- 4572Da^2 \text{Pr} Rd (\cos\gamma)^2 \alpha_2^2 \alpha_3 - 17145Da^2 \text{Pr} (\cos\gamma)^2 \phi^4 \alpha_2^2 \alpha_3 - 120Da^2 (1-\phi)^{5/2} Rd (\cos\gamma)^2 \alpha_1 \alpha_2^2 \\ &- 3024Da^2 (1-\phi)^{5/2} \text{Pr} Rd \alpha_1 \alpha_3 + 225Da^2 (1-\phi)^{5/2} (\cos\gamma)^2 \phi \alpha_1 \alpha_2^2 + 600Da^2 (1-\phi)^{5/2} Rd (\cos\gamma)^2 \phi \alpha_1 \alpha_2^2 \\ &- 1200Da^2 (1-\phi)^{5/2} Rd (\cos\gamma)^2 \phi^2 \alpha_1 \alpha_2^2 + 1200Da^2 (1-\phi)^{5/2} Rd (\cos\gamma)^2 \phi^3 \alpha_1 \alpha_2^2 \\ &- 600Da^2 (1-\phi)^{5/2} Rd (\cos\gamma)^2 \phi^4 \alpha_1 \alpha_2^2 + 120Da^2 (1-\phi)^{5/2} Rd (\cos\gamma)^2 \phi^5 \alpha_1 \alpha_2^2 + 16Rd^2 \\ &+ 9Da^2 M^4 - 288Da(1-\phi)^{5/2} Rd \alpha_1 - 108Da^2 M^2 (1-\phi)^{5/2} \alpha_1 + 1560Da^2 Rd \phi \alpha_1^2 \\ &- 117Da^2 \alpha_1^2 - 3429Da^2 \text{Pr} (\cos\gamma)^2 \alpha_2^2 \alpha_3 + 17145Da^2 \text{Pr} (\cos\gamma)^2 \phi \alpha_2^2 \alpha_3 \\ &+ 400Da^2 (1-\phi)^{5/2} Rd^2 (\cos\gamma)^2 \phi \alpha_1 \alpha_2^2 + 36DaM^2 a + 800Da^2 (1-\phi)^{5/2} Rd^2 (\cos\gamma)^2 \phi^3 \alpha_1 \alpha_2^2 \\ &- 800Da^2 (1-\phi)^{5/2} Rd^2 (\cos\gamma)^2 \phi^2 \alpha_1 \alpha_2^2 + 80Da^2 (1-\phi)^{5/2} Rd^2 (\cos\gamma)^2 \phi^5 \alpha_1 \alpha_2^2 - 400Da^2 (1-\phi)^{5/2} Rd^2 (\cos\gamma)^2 \phi^4 \alpha_1 \alpha_2^2 \\ &- 45720Da^2 \text{Pr} Rd b (\cos\gamma)^2 \phi^2 \alpha_2^2 \alpha_3 + 22860Da^2 \text{Pr} Rd b \cos\gamma^2 \phi \alpha_2^2 \alpha_3 + 4572Da^2 \text{Pr} Rd b \cos\gamma^2 \phi^5 \alpha_2^2 \alpha_3 \\ &- 22860Da^2 \text{Pr} Rd (\cos\gamma)^2 \phi^4 \alpha_2^2 \alpha_3 + 45720Da^2 \text{Pr} Rd (\cos\gamma)^2 \phi^3 \alpha_2^2 \alpha_3 - 3120Da^2 Rd \phi^2 \alpha_1^2 + 3120Da^2 Rd \phi^3 \alpha_1^2 \\ &- 1560Da^2 Rd \phi^4 \alpha_1^2 + 312Da^2 Rd \phi^5 \alpha_1^2 + 1040Da^2 Rd^2 \phi \alpha_1^2 + 22680Da^2 \text{Pr}^2 a^3 \alpha_3^2 + 24Rd \\ &+ 2080Da^2 Rd^2 \phi^3 \alpha_1^2 - 2080Da^2 Rd^2 a^3 \phi^2 \alpha_1^2 - 1040Da^2 Rd^2 \phi^4 \alpha_1^2 - 192Da(1-\phi)^{5/2} Rd^2 \alpha_1 \\ &+ 208Da^2 Rd^2 \phi^5 \alpha_1^2 - 312Da^2 Rd \alpha_1^2 + 32DaM^2 Rd^2 + 16Da^2 M^4 Rd^2 - 208Da^2 Rd^2 \alpha_1^2 \end{aligned} \right)
 \end{aligned}$$

The functions in Eq. (33) and (34) and that in Eq. (38) and (39) have relations as follows:

$$\theta(\eta) = b^r \mathcal{G}(b^s \eta) \rightarrow \theta(\infty) = b^r \mathcal{G}(\infty) \quad (41)$$

$$f(\eta) = a^k g(a^q \eta) \rightarrow f'(\eta) = a^{k+q} g'(a^q \eta) \rightarrow f'(\infty) = a^{k+q} g'(\infty) \quad (40)$$

From Eq. (12),  $f'(\infty)=0$  and  $\theta(\infty)=0$

Since  $a \neq 0$  and  $b \neq 0 \rightarrow g'(\infty)=0$  and  $\mathcal{G}(\infty)=0$

and

## Applying multi-step DTM

To solve the boundary layer problems, the domain  $[0, \infty)$  is replaced by  $[0, \eta_\infty]$ . But  $\eta_\infty$  should be great enough that the solution is

not dependent on. The solution domain should be divided to  $N$  equal parts ( $H = \eta_\infty/N$ ). So, we have

$$g_i'''(\eta_i) + (1-\phi)^{2.5} \left\{ \left[ (1-\phi) + \phi \left( \frac{\rho_s}{\rho_f} \right) \right] \left( 3g_i(\eta_i)g_i''(\eta_i) - 2(g_i'(\eta_i))^2 \right) + \left[ (1-\phi) + \phi \left[ (\rho\beta)_s / (\rho\beta)_f \right] \right] g_i(\eta_i) \cos\gamma - (M^2 + Da^{-1})g_i(\eta_i) \right\} = 0 \quad (42)$$

$$(i-1)H \leq \eta_i < iH, \quad \text{for } i \leq N$$

$$g_i''(\eta_i) + 3 \left[ \frac{1}{(1-\phi) + \phi \left[ (\rho C_p)_s / (\rho C_p)_f \right]} \right] \left[ \frac{k_s + (m-1)k_f - (m-1)\phi(k_f - k_s)}{k_s + (m-1)k_f + \phi(k_f - k_s)} \right] Pr g_i(\eta_i) g_i'(\eta_i) = 0 \quad (43)$$

$$(i-1)H \leq \eta_i < iH, \quad \text{for } i \leq N$$

Applying multi-step DTM on Eq. (42) and Eq. (43)

$$G_i(p+3) = \frac{(1-\phi)^{2.5} H^3}{(p+1)(p+2)(p+3)} \left\{ \alpha_1 \left[ \frac{2 \sum_{l=0}^p \frac{(l+1)}{H} G_i(l+1) \frac{(p-l+1)}{H} G_i(p-l+1)}{-3 \sum_{l=0}^p G_i(l) \frac{(p-l+1)(p-l+2)}{H^2} G_i(p-l+2)} \right] - \alpha_2 g_i(p) \cos\gamma - (M^2 + Da^{-1})G_i(p) \right\}$$

$$\text{for } i \leq N \quad (44)$$

$$g_i(p+2) = \frac{-3H^2 Pr}{(p+1)(p+2)} \left\{ \alpha_3 \sum_{l=0}^p \frac{(l+1)}{H} g_i(l+1) G_i(p-l) \right\} \quad (45)$$

$$\text{for } i \leq N$$

The initial conditions for the problem are considered for the first sub domain ( $i=1$ ). Following Eq. (24), the differential transform for the initial conditions for Eq. (35) and (36) and for Eqs. (44) and (45) are

$$G_1(0) = g_1(0) = 0, \quad G_1(1) = H g_1'(0) = 0, \quad G_1(2) = \frac{H^2}{2} g_1''(0) = \frac{H^2}{2},$$

$$\Psi_1(0) = g_1'(0) = 1, \quad \Psi_1(1) = H g_1''(0) = H \quad (46)$$

The boundary conditions of each subdomain are continuity of the

$$g_i(\eta_i), \quad g_i'(\eta_i), \quad g_i''(\eta_i), \quad g_i(\eta_i), \quad \text{and } g_i'(\eta_i) \quad (47)$$

These boundary conditions can be obtained from Eq. (26):

$$g_i(\eta_{i+1}) = \sum_{k=0}^m G_i(k) \quad (48a)$$

$$g_{i+1}(\eta_{i+1}) = G_{i+1}(0) \rightarrow G_{i+1}(0) = \sum_{k=0}^m G_i(k)$$

$$g_i'(\eta_{i+1}) = \sum_{k=1}^m \frac{k}{H} G_i(k)$$

$$g_i'(\eta_{i+1}) = \frac{G_{i+1}(1)}{H} \rightarrow G_{i+1}(1) = \sum_{k=1}^m k G_i(k) \quad (48b)$$

$$g_i''(\eta_{i+1}) = \sum_{k=2}^m \frac{k(k-1)}{H^2} G_i(k)$$

$$g_i''(\eta_{i+1}) = \frac{2G_{i+1}(2)}{H^2} \rightarrow G_{i+1}(2) = \frac{1}{2} \sum_{k=2}^m k(k-1) G_i(k) \quad (48c)$$

$$g_i(\eta_{i+1}) = \sum_{k=0}^m \Psi_i(k)$$

$$g_{i+1}(\eta_{i+1}) = \Psi_{i+1}(0) \rightarrow \Psi_{i+1}(0) = \sum_{k=0}^m \Psi_i(k) \quad (49a)$$

$$g_i'(\eta_{i+1}) = \sum_{k=1}^m \frac{k}{H} \Psi_i(k)$$

$$g_i'(\eta_{i+1}) = \frac{\Psi_{i+1}(1)}{H} \rightarrow \Psi_{i+1}(1) = \sum_{k=1}^m k \Psi_i(k) \quad (49a)$$

The values of the  $g'(\eta_\infty)$  and  $g(\eta_\infty)$  can be calculated by differentiating from Eq. (24)

$$g_i'(\infty) \approx g_i'(\eta_\infty) = g_i'(\eta_{N+1}) = \sum_{k=1}^m \frac{k}{H} G_N(k)$$

$$g_i(\infty) \approx g_i(\eta_\infty) = g_i(\eta_{N+1}) = \sum_{k=0}^m \Psi_N(k) \quad (50)$$

Now, Eq. (11) and (12) are solved with a similar process like Eqs. (35) and (36) using multi-step DTM. The only difference is that the condition  $f''(0) = a$  is replaced by the condition  $g''(0) = 1$

It should be noted as mentioned previously that the unknown parameters “ $a$ ” and “ $b$ ” in the solutions are unknown constants. The infinite boundary conditions i.e.  $\eta \rightarrow \infty$ ,  $f' = 0$ ,  $\theta = 0$  are applied.

The resulting simultaneous equations are solved to obtain the values of “ $a$ ” and “ $b$ ” for the respective values of the physical and thermal properties of the nanofluids under considerations (Figures1–4).

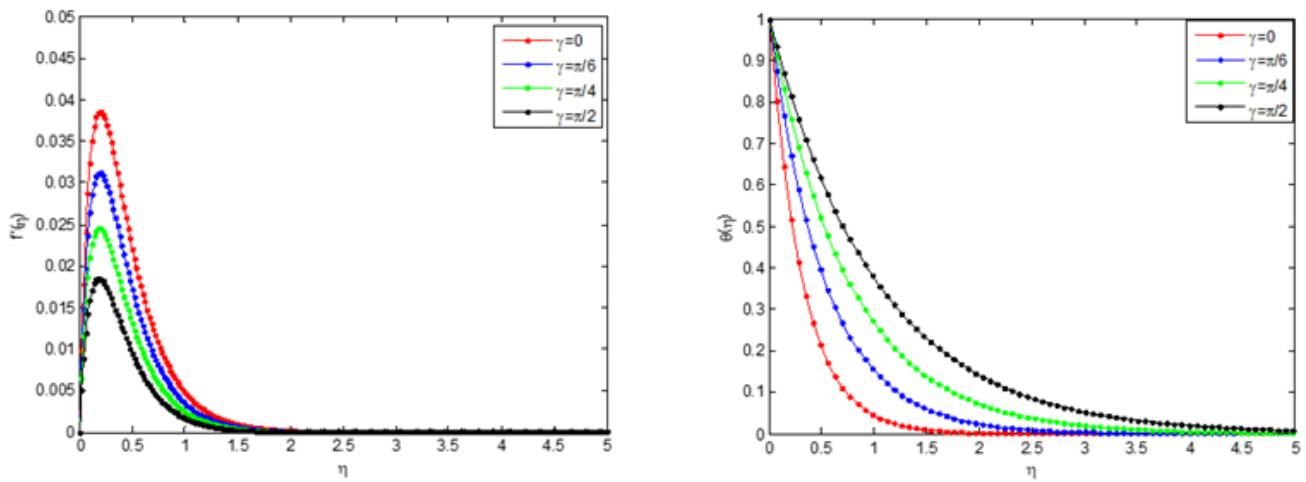


Figure 2 (a) Effects of cone angle on the velocity profile, (b) Effects of cone angle on temperature profile.

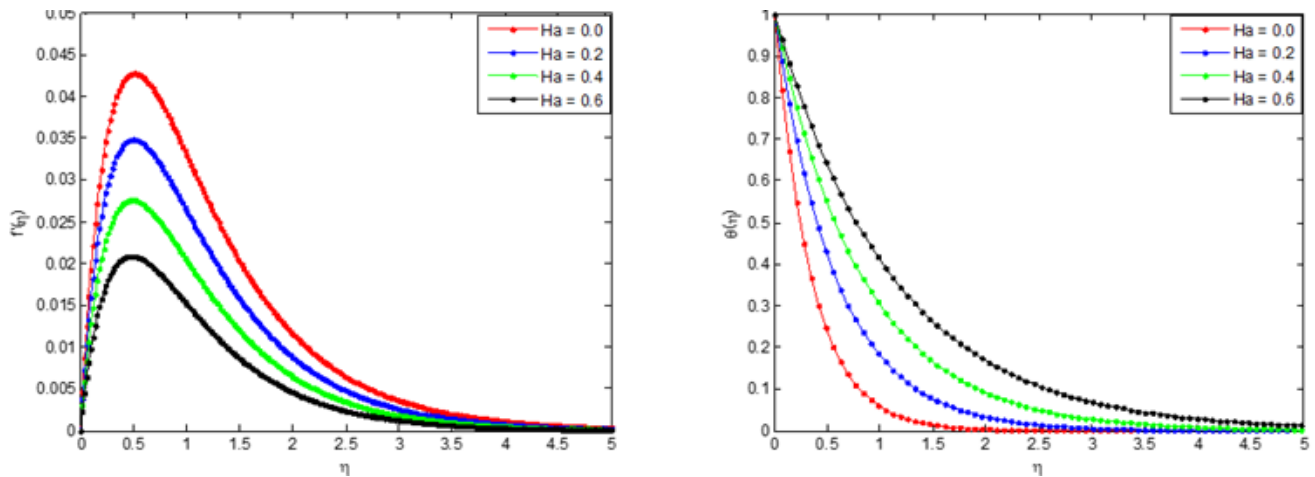


Figure 3 (a) Effects of magnetic field on the velocity profile, (b) Effects of magnetic field on temperature profile.

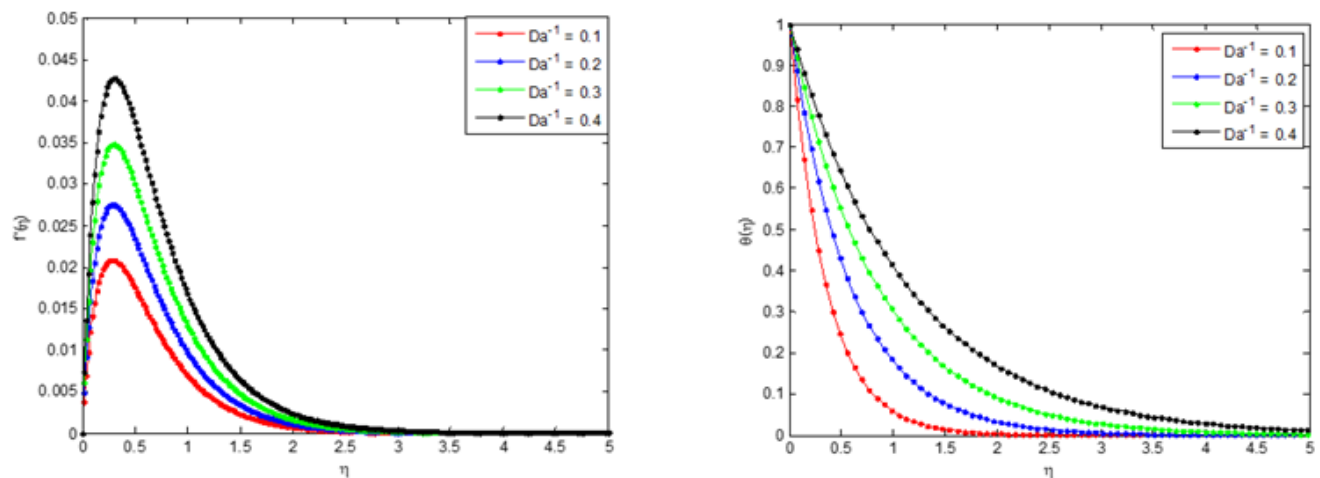


Figure 4 (a) Effects of flow medium porosity on the velocity profile, (b) Effects of flow medium porosity on temperature profile.

## Flow and heat transfer parameters

The determinations of other physically important quantities such as shear stress, drag, heat transfer rate and heat transfer coefficient) associated with the free convection flow and heat transfer problem are very important in the design of equipment. Therefore, in this analysis physically important quantities are computed. The local heat transfer coefficient at the surface of the vertical plate can be obtained from

### Fluid flow parameter

Skin friction coefficient

$$c_f = \frac{\tau_w}{\rho_{nf} u^2} = \frac{\mu_{nf} \left. \frac{\partial u}{\partial y} \right|_{y=0}}{\rho_{nf} u^2} = \frac{\mu_{nf} \left( \frac{\partial u}{\partial \eta} \cdot \frac{\partial \eta}{\partial y} \right) \Big|_{y=0}}{\rho_{nf} u^2} \quad (51)$$

The dimensionless form of the skin friction coefficient,

$$c_f (Re_x)^{1/2} = \frac{f''(0)}{(1-\phi)^{2.5}}$$

$$c_f (Re_x)^{1/2} \frac{\tau_w}{(4Gr_x^3)^{1/4} (\nu\mu)} = f''(0) \frac{f''(0)}{(1-\phi)^{2.5}} \quad (52)$$

### Heat transfer parameter

$$h_x = -\frac{k_{nf}}{T_w - T_\infty} \left( \frac{\partial T}{\partial y} \right)_{y=0} = -k_{nf} \theta'(0) \frac{1}{x} \left( \frac{1}{4} Gr_x \right)^{1/4} \quad (53)$$

### The local nusselt number

The local Nusselt number is

$$Nu_x = \frac{h_x x}{k_{nf}} = -\left( \frac{x}{T_w - T_\infty} \right) \left( \frac{\partial T}{\partial y} \right)_{y=0} = -\theta'(0) \left( \frac{1}{4} Gr_x \right)^{1/4}$$

$$Nu_x = -\frac{\theta'(0)}{\sqrt{2}} Gr_x^{1/4} = f((Pr) Gr_x^{1/4}) \quad (54)$$

where  $\phi(Pr) = -\frac{\theta'(0)}{\sqrt{2}}$  is a function of Prandtl number. The dependence of  $\phi$  on the Prandtl number is evidenced by Eq. (54).

It could also be shown that

$$\frac{Nu_x}{(Re_x)^{1/2}} = -\frac{k_{nf}}{k_f} \theta'(0) = -\left[ \frac{k_s + (m-1)k_f - (m-1)\phi(k_f - k_s)}{k_s + (m-1)k_f + \phi(k_f - k_s)} \right] \theta'(0) \quad (55)$$

where  $Re_x$  and  $Gr_x$  are the local Reynold and Grashof numbers defined as:

$$Re_x = \frac{ux}{\nu_{nf}} \quad \text{and} \quad Gr_x = \frac{g\beta(T_w - T_\infty)x^3}{\nu^3}$$

## Results and discussion

Tables 5–7 present various comparisons of results of the present study and the past works for viscous fluid i.e. when the volume fraction of the nanoparticle is zero ( $\phi=0$ ). Also, setting half of the cone angle

to infinity, i.e.  $\gamma \rightarrow \infty$ , and neglecting the magnetic effects. It could be seen from the Tables that there are excellent agreements between the past results and the present study. Moreover, the Tables present the effects of Prandtl number on the flow and heat transfer processes.

**Table 5** Comparison of results for the skin friction parameter

$f''(0)$			
Pr	Sparrow & Gregg <sup>5</sup>	Kuiken <sup>8</sup>	Present Study
0.003	1.0223	1.0151	1.0224
0.008	0.9955	0.9801	0.9955
0.02	0.959	0.9284	0.9591
0.03	0.9384	0.8966	0.9384

**Table 6** Comparison of results of  $f(\infty)$

$f(\infty)$			
Pr	Sparrow & Gregg <sup>5</sup>	Kuiken <sup>8</sup>	Present Study
0.003	8.7060	8.8763	8.7061
0.008	5.4018	5.4152	5.4018
0.020	3.4093	3.4055	3.4093
0.030	2.7878	2.7710	2.7878

**Table 7** Comparison of results of  $-\theta'(0)$

$Nu_x / (G_x Pr^2)^{1/4} = -\theta'(0)$			
Pr	Sparrow & Gregg <sup>5</sup>	Kuiken <sup>8</sup>	Present Study
0.003	0.5827	0.5827	0.5827
0.008	0.5729	0.5714	0.5728
0.020	0.5582	0.5546	0.5582
0.030	0.5497	0.5443	0.5497

## Effect of cone angle on nanofluid velocity and temperature distributions

The variations of the flow velocity and the temperature gradient of the fluid are inversely proportional to half of the cone angle,  $\gamma$  increases. It should be noted that as the angle increases, the applied magnetic field decreases. Also, the skin friction factor in terms of shear stress and heat transfer rate in terms of Nusselt number are decreased.

Figure 5 shows the effects of magnetic parameter on the fluid velocity and the temperature. As in the preceding parametric study, the fluid velocity and the temperature decrease as the magnetic field increases. This is because, magnetic field creates a flow resistance force called Lorentz force in the flow. The presence of this force in the flow slows fluid motion at boundary layer on solid walls. Consequently, there is decrease the fluid velocity and increase fluid temperature within the boundary layer. And by extension, the skin friction factor in terms of shear stress and heat transfer rate in terms of Nusselt number are decreased.

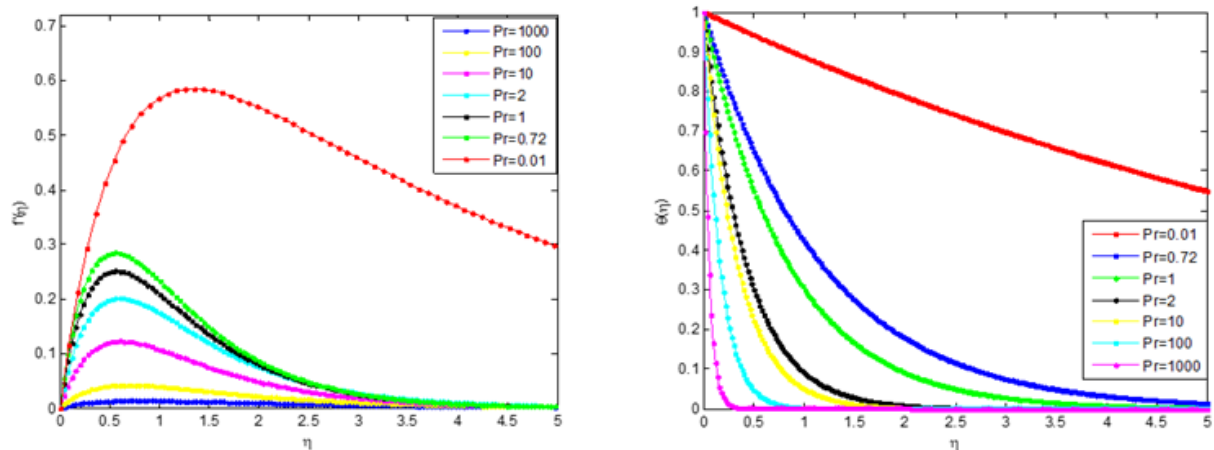


**Figure 5** (a) Effects of Prandtl number on the velocity profile when  $\phi=0.020$ , (b) Effects of Prandtl number on temperature profile when  $\phi=0.020$ .

### Effect of flow medium porosity on nanofluid velocity and temperature distributions

Effects of Darcy number which represent flow medium porosity parameter on the flow velocity and temperature distributions are

presented in Figure 6. It is depicted in the figure that as the porosity parameter increases the flow velocity of the fluid decrease while the temperature distribution in the flow increases as the Darcy number increases.

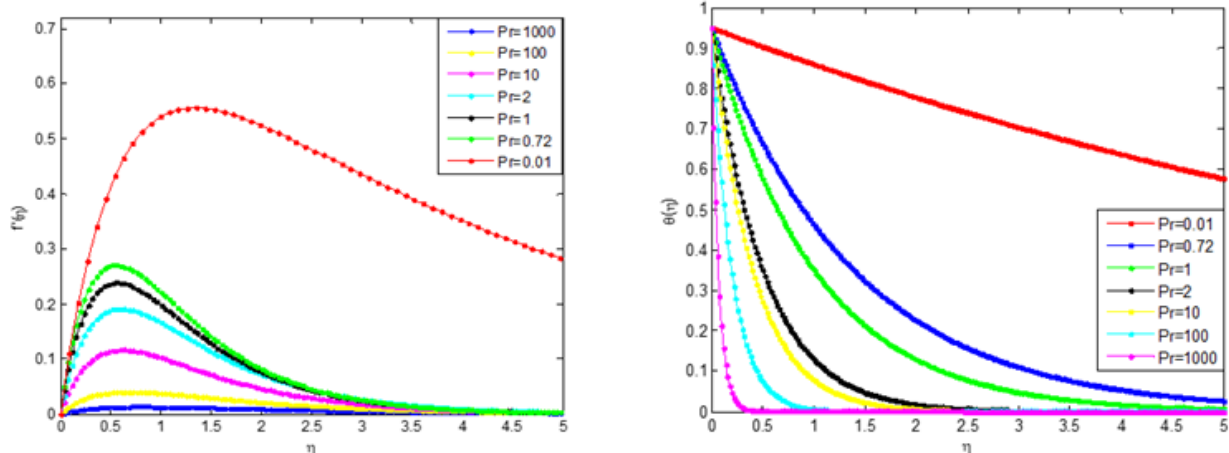


**Figure 6** (a) Effects of Prandtl number on the velocity profile when  $\phi=0.040$ , (b) Effects of Prandtl number on temperature profile when  $\phi=0.040$ .

### Effect of nanoparticle volume fraction on the velocity and temperature distributions

It has been shown in some previous studies that the presence of nanoparticles in a fluid has significant effects on the flow behaviours of fluid. Figures 7&8 show the effects nanoparticle concentration/volume fraction and Prandtl number on velocity and temperature profiles of copper (II) oxide-water nanofluid. It is indicated in the Figures that as the volume-fraction or concentration of the nanoparticle in the nanofluid increases, the velocity decreases. However, an opposite trend in the temperature profile is observed i.e. the nanofluid temperature increases as the volume-fraction of the nanoparticles in the basefluid increases. This is because, the solid volume fraction has significant impacts on the thermal conductivity. The increased volume fraction of nanoparticles in basefluid results in higher thermal conductivity of the basefluid which increases the heat enhancement capacity of the basefluid. Also, one of the possible reasons for the enhancement on heat transfer of nanofluids can be explained by the high concentration of nanoparticles in the thermal

boundary layer at the wall side through the migration of nanoparticles. It should also be stated that the thickness of thermal boundary layer rises with increasing the values of nanoparticle volume fraction. This consequently reduces the velocity of the nanofluid as the shear stress and skin friction are increased.

Furthermore, the figures show the effects of Prandtl number ( $Pr$ ) on the velocity and temperature profiles. It is indicated that the velocity of the nanofluid decreases as the  $Pr$  increases but the temperature of the nanofluid increases as the  $Pr$  increases. This is because the nanofluid with higher Prandtl number has a relatively low thermal conductivity, which reduces conduction, and thereby reduces the thermal boundary-layer thickness, and as a consequence, increases the heat transfer rate at the surface. For the case of the fluid velocity that decreases with the increase of  $Pr$ , the reason is that fluid of the higher Prandtl number means more viscous fluid, which increases the boundary-layer thickness and thus, reduces the shear stress and consequently, retards the flow of the nanofluid. Also, it can be seen that the velocity distribution for small value of Prandtl number consist

of two distinct regions. A thin region near the wall of the plate where there are large velocity gradients due to viscous effects and a region where the velocity gradients are small compared with those near the wall. In the later region, the viscous effects are negligible and the

flow of fluid in the region can be considered to be inviscid. Also, such region tends to create uniform accelerated flow at the surface of the plate.

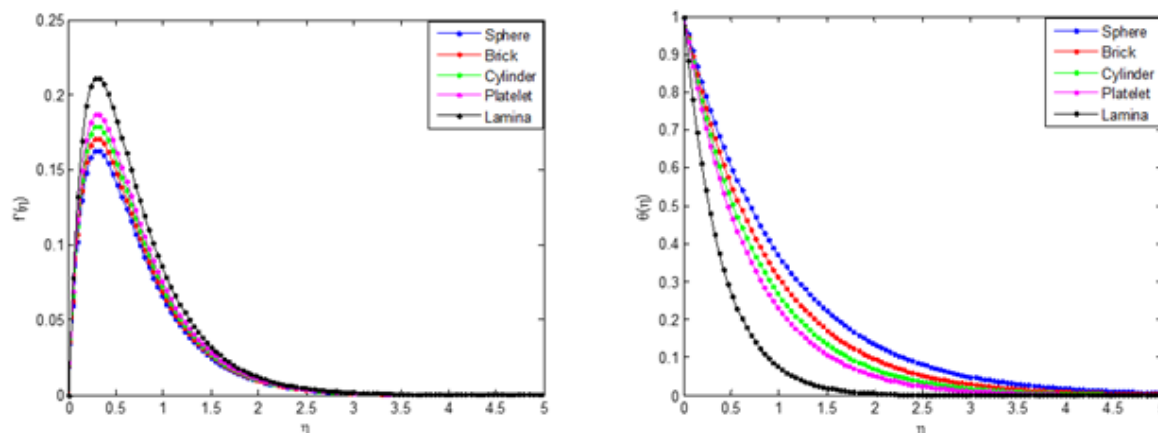


**Figure 7(a)** Effect of nanoparticle shape on velocity distribution of the nanofluid, **(b)** Effects of nanoparticle shape on temperature distribution of nanofluid.

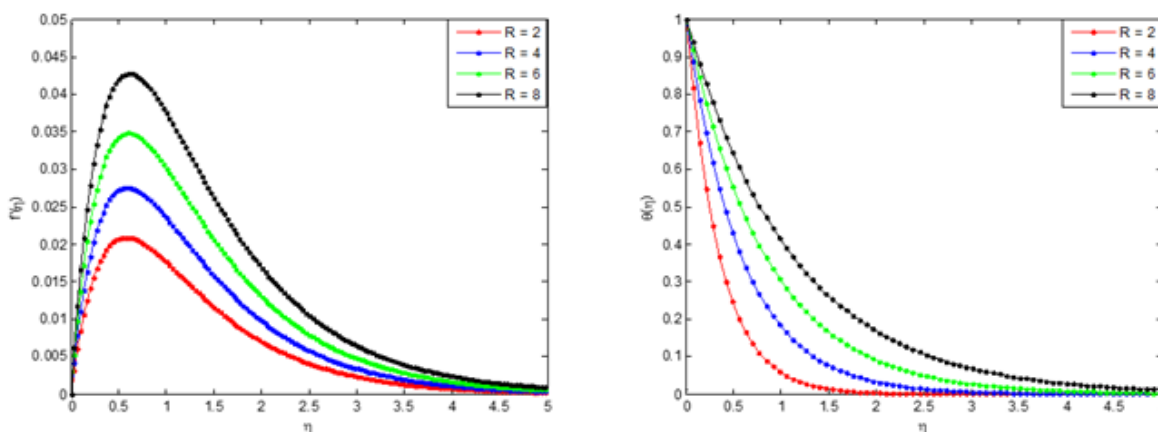


**Figure 8 (a)** Effects of radiation parameter on the velocity profile of the nanofluid, **(b)** Effects of radiation parameter on temperature profile of the nanofluid.

It is shown in this study that the use of nanoparticles in the fluid exhibited better properties relating to the heat transfer of fluid than heat transfer enhancement through the use of suspended millimeter- or micrometer-sized particles which potentially cause some severe problems, such as abrasion, clogging, high pressure drop, and sedimentation of particles. The very low concentrations applications and nanometer sizes properties of nanoparticles in basefluid prevent the sedimentation in the flow that may clog the channel. It should be added that the theoretical prediction of enhanced thermal conductivity of the basefluid and prevention of clogging, abrasion, high pressure drop and sedimentation through the addition of nanoparticles in basefluid have been supported with experimental evidences in literature.

### Effect of nanoparticle shape on the velocity and temperature distributions

The impact of nanoparticle shape at different values of Prandtl number on velocity and temperature profiles of Copper (II) Oxide-water nanofluid is shown in Figure 9. It is indicated that the maximum decrease in velocity and maximum increase in temperature are caused by lamina, platelets, cylinder, bricks and sphere, respectively. It is observed that lamina shaped nanoparticle carries maximum velocity whereas spherical shaped nanoparticle has better enhancement on

heat transfer than other nanoparticle shapes. This is because the lamina nanoparticle has greater shape factor than other nanoparticles of different shapes. The enhancement observed at lower volume fractions for non-spherical particles is attributed to the percolation chain formation, which perturbs the boundary layer and thereby increases the local Nusselt number values.

It is evident from this study that proper choice of nanoparticles will be helpful in controlling velocity and heat transfer. It is also observed that irreversibility process can be reduced by using nanoparticles, especially the spherical particles. This can potentially result in higher enhancement in the thermal conductivity of a nanofluid containing elongated particles compared to the one containing spherical nanoparticle, as exhibited by the experimental data in the literature.

### Effect of thermal radiation parameter on the velocity and temperature distributions

The variation in the thermal radiation parameter is directly proportional to the velocity of the fluid to increase. This is because as the radiation parameter is augmented, the absorption of radiated heat from the heated plate releases more heat energy released to the fluid and the resulting temperature increases the buoyancy forces in the boundary layer which also increases the fluid motion and the

momentum boundary layer thickness accelerates. This is expected, because the considered radiation effect within the boundary layer increases the motion of the fluid which increases the surface frictions.

The influence of radiation parameter on the temperature field is illustrated in Figure 11. Increase in the radiation parameter contributes in general to increase in the temperature of the nanofluid. This is because, as the thermal radiation increases, the absorption of radiated heat from the heated plate releases heat energy released to the fluid the thermal boundary layer of fluid increases as the temperature near the boundary is enhanced.

## Conclusion

The analysis of magnetohydrodynamics natural convection of nanofluid flow over a vertical circular cone immersed in a porous medium under the influence of thermal radiation have been carried out in this work using multi-step differential transformation method. Effects of various parameters of the flow and heat transfer models on the fluid-dynamic and thermal behaviours of the nanofluid have been examined and discussed using the approximate analytical solutions. Also, the accuracies of the developed analytical solutions were evaluated by comparing the results of the present study with the results of the numerical solutions and the past studies. It is believed that this study will create a better physical insight into the flow process for the design of flow and heat transfer equipment.

## Acknowledgments

None.

## Conflicts of interest

There are no conflicts of interest.

## Funding

None.

## References

- Schmidt E, Beckmann W. The temperature and speed field in front of a heat-emitting vertical plate at a natural convection. *Tech Mech U Thermodynamik*. 1930;1(10):341–349.
- Ostrach S. An analysis of laminar free-convection flow and heat transfer about a flat plate parallel to the direction of the generating body force. NACA Report. 1953. 1111 p.
- Sparrow EM, JL Gregg. Laminar free convection from a vertical plate with uniform surface heat flux in chemically reacting systems. *Trans A.S.M.E.* 1956;45(2):435–440.
- Lefevre EJ. Laminar free convection from a vertical plane surface, 9th Intern. Congress on Applied Mechanics. Brussels; 1956. 168 p.
- Sparrow EM, Gregg JL. Similar solutions for free convection from a nonisothermal vertical plate. *Trans A.S.M.E.* 1958;80:379–386.
- Stewartson K, LT Jones. The heated vertical plate at high Prandtl number. *J Aeronautical Sciences*. 1957;24:379–380.
- Kuiken HK. An asymptotic solution for large Prandtl number free convection. *J Engng Math*. 1968;2:355–371.
- Kuiken HK. Free convection at low Prandtl numbers. *J Fluid Mech*. 1969;37:785–798.
- Eshghy S. Free-convection layers at large Prandtl number. *J Applied Math Physics (ZAMP)*. 1971;22:275–292.
- S. Roy, High Prandtl number free convection for uniform surface heat flux. *Trans A.S.M.E.J Heat Transfer*. 1973;95:124–126.
- Kuiken HK, Z Rotem. Asymptotic solution for the plume at very large and small Prandtl numbers. *J Fluid Mech*. 1971;45:585–600.
- TY Na, IS Habib. Solution of the natural convection problem by parameter differentiation. *Int J Heat Mass Transfer*. 1974;17(3):457–459.
- Merkin JH. A note on the similarity solutions for free convection on a vertical plate. *J Engng Math*. 1985;19:189–201.
- Merkin JH, Pop I. Conjugate free convection on a vertical surface. *Int J Heat Mass Transfer*. 1996;39:1527–1534.
- Ali FM, R Nazar, NM Arifin. Numerical investigation of free convective boundary layer in a viscous fluid. *The American Journal of Scientific Research*. 2009;5:13–19.
- SS Motsa, S Shateyi, Z Makukula. Homotopy analysis of free convection boundary layer flow with heat and mass transfer. *Chemical Engineering Communications*. 2011;198(6):783–795.
- SS Motsa, ZG Makukula, S Shateyi. Spectral Local Linearisation Approach for Natural Convection Boundary Layer Flow. *Hindawi Publishing Corporation Mathematical Problems in Engineering*. 2013;765013:7.
- AR Ghotbi, H Baramia, G Domairry, et al. Investigation of a powerful analytical method into natural convection boundary layer flow. *Communications in Nonlinear Science and Numerical Simulation*. 2009;14(5):2222–2228.
- JK Zhou. Differential Transformation and Its Applications for Electrical Circuits. Huazhong University Press, Wuhan, China; 1986.
- LT Yu, CK Chen. The solution of the Blasius equation by the differential transformation method. *Math Comput Modell*. 1998;28(1):101–111.
- BL Kuo. Thermal boundary-layer problems in a semi-infinite flat plate by the differential transformation method. *Appl Math Comput*. 2004;150(2):143–160.
- BL Kuo. Application of the differential transformation method to the solutions of the free convection problem. *Applied Mathematics and Computation*. 2005;165:63–79.
- MM Rashidi, N Laraqi, SM Sadri. A Novel Analytical Solution of Mixed Convection about an Inclined Flat Plate Embedded in a Porous Medium Using the DTM-Pade. *International Journal of Thermal Sciences*. 2010;49(12):2405–2412.
- ER El-Zahar. Applications of adaptive multi-step differential transform method to singular perturbation problems arising in science and engineering. *Applied Math Inf Sci*. 2015;9:223–232.
- VS Erturk, ZM Odibat, S Momani. The multi-step differential transform method and its application to determine the solutions of nonlinear oscillators. *Adv Applied Math Mechan*. 2012;4:422–438.
- Gokdogan A, M Merdan, A Yildirim. Adaptive multi-step differential transformation method to solving nonlinear differential equations. *Math Comput Modell*. 2012a;55:761–769.
- Gokdogan A, M Merdan, A Yildirim. A multistage differential transformation method for approximate solution of Hantavirus infection model. *Commun Nonlinear Sci Numerical Simulat*. 2012b;17:1–8.
- MM Alam, MA Alim, MK Chowdhury. Free convection from a vertical permeable circular cone with pressure work and non-uniform surface temperature. *Nonlinear Analysis Modeling and Control*. 2007;261:21–32.
- Alamgir M. Over-all Heat Transfer from Vertical Cones in Laminar Free Convection: An Approximate Method, Transactions of ASME. *J Heat Transfer*. 1979;101:174–176.

30. MA Alim, MM Alam, MK Chowdhury. Pressure work effect on natural convection from a vertical circular cone with suction and non-uniform surface temperature. *Mech Eng*. 2014;36:6–11.
31. EMA Elbashbeshy, TG Emam, EA Sayed. Effect of pressure work on free convection flow from a vertical circular cone with variable surface heat flux. *Strojnicky casopis*. 2012;63(3):169–177.
32. RG Hering, RJ Grosh. Laminar free convection from a non-isothermal cone. *Int Heat Mass Transfer*. 1962;5:1059–1068.
33. MA Hossain, SC Paul. Free convection from a vertical permeable circular cone with non-uniform surface heat flux. *Heat Mass Transfer*. 2001;37:167–173.
34. TY Na, JP Chiou. Laminar Natural Convection over a frustum of a Cone. *Appl Sci Res*. 1979;35:409–421.
35. S Roy. Free convection over a slender vertical cone at high Prandtl numbers. *ASME J Heat Mass Transfer*. 1974;101:174–176.
36. EMA Elbashbeshy, TG Emam, EA Sayed. Effect of pressure work on free convection flow about a truncated cone. *International Journal of Physical Sciences*. 2011;1(1):001–010.
37. Akbar NS, AW Butt. Ferro-magnetic effects for peristaltic flow of Cu-water nanofluid for different shapes of nano-size particles. *Appl Nanosci*. 2016;6:379–385.
38. Sheikholesmi M, MM Bhatti. Free convection of nanofluid in the presence of constant magnetic field considering shape effects of nanoparticles. *International Journal of Heat and Mass Transfer*. 2017;111:1039–1049.
39. Ul Haq R, Nadeem S, ZH Khan, et al. Convective heat transfer in MHD slip flow over a stretching surface in the presence of carbon nanotubes. *Physica B*. 2015;457:40–47.
40. Talley LD, GL Pickard, WJ Emery, et al. Descriptive Physical Oceanography. Physical Properties of Sea Water. 6th ed. Elsevier Ltd; 2011. p. 2–6M5.
41. Pastoriza-Gallego M, L Lugo, J Legido, et al. Thermal conductivity and viscosity measurements of ethylene glycol-based Al<sub>2</sub>O<sub>3</sub> nanofluids. *Nanoscale Res Lett*. 2011;6(221):1–11.
42. Aberoumand S, A Jafarimoghaddam. Experimental study on synthesis, stability, thermal conductivity and viscosity of Cu–engine oil nanofluid. *Journal of the Taiwan Institute of Chemical Engineers*. 2017;71:315–322.
43. Kuiken HK. On boundary layers in fluid mechanics that decay algebraically along stretches of wall that are not vanishingly small, IMA. *Journal of Applied Mathematics*. 1981;27(4):387–405.
44. Thameem Basha H, IL Animasaun, OD Makinde, et al. Effect of Electromagnetohydrodynamic on Chemically Reacting Nanofluid Flow over a Cone and Plate. Applied Mathematics and Scientific Computing. Trends in Mathematics. *Birkhäuser Cham*. 2019;99–107.